



Cape Peninsula  
University of Technology

**EVALUATION OF CORROSION PRODUCT TRANSPORT IN THE SECONDARY  
PLANT OF A PRESSURISED WATER REACTOR**

by

**MALEKE MOSES MONTSHIWAGAE**

**Thesis submitted in fulfilment of the requirements for the degree**

**Master of Technology: Chemistry**

**in the Faculty of Applied Science**

**at the Cape Peninsula University of Technology**

**Supervisor: Prof Tjaart van der Walt**

**Co-supervisor: Dr Nestor van Eeden**

**Bellville**

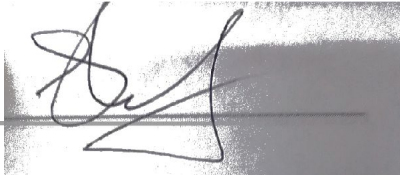
Date submitted: February 2018

**CPUT copyright information**

The dissertation/thesis may not be published either in part (in scholarly, scientific or technical journals), or as a whole (as a monograph), unless permission has been obtained from the University

## DECLARATION

I, Maleke Moses Montshiwagae, declare that the contents of this dissertation/thesis represent my own unaided work, and that the dissertation/thesis has not previously been submitted for academic examination towards any qualification. Furthermore, it represents my own opinions and not necessarily those of the Cape Peninsula University of Technology.



Signed

11/09/2023

Date

## ABSTRACT

In this study, the total amount of transported iron corrosion products during startup was evaluated. This was done by simultaneous collection of particulate and soluble iron samples using a 0.45  $\mu\text{m}$  nitro-cellulose and a 0.45  $\mu\text{m}$  resin impregnated filters respectively. Samples were collected at predetermined frequencies of 2 hrs, 4 hrs, 8 hrs, 16 hrs, 24 hrs and 48 hrs below 30 % reactor power, followed by 11 days startup basis after which a 7 days sampling period was followed for the entire duration of the fuel cycle.

Samples were acid digested followed by determination of total iron concentrations using atomic absorption spectrophotometer (flame). The results were used to estimate iron transport amounts for each sampling period, from which a cumulative curve was constructed, and a regression equation worked out. The startup transport amounts for < 30 % reactor power period defined as time zero and for a defined period of 11 days were determined to be 5.443 kg (+/- 1.709) and 4.08 kg respectively, giving a total startup amount of about 9.84 kg.

Based on comparison with other nuclear power plants, it was concluded that 9.84 kg is within the range as reported across industry and as such, the current startup practices with respect to their effect on corrosion product transport are generally of no concern. It was further concluded that, it is important to establish adequate redox chemistry conditions early in the startup period to promote magnetite ( $\text{Fe}_3\text{O}_4$ ) formation to minimize iron transport.



## ACKNOWLEDGEMENTS

### I wish to thank:

- Prof Nico Tjaart van der Walt, for his patience and understanding through the past few years, his academic guidance and leadership that led to the completion of this thesis.
- Dr Nestor van Eeden, for his continuous mentoring and academic guidance and input throughout this journey up to the completion of this thesis.
- Koeberg chemistry staff members, Mr Desmond Visagie, Abe Hendricks and Siviwe Makade for their efforts in collecting the samples. Mrs Lolita Laubscher for carrying out the chemical analysis in the laboratory.
- Mr Ashley Fortuin (former chemistry manager), for supporting my request for studying and allowing the use of both human and Eskom laboratory resources.
- My son and daughter for inspiring me to complete this thesis.
- My mother for her great support.
- Eskom for provision of the study bursary.

## **DEDICATION**

**To:** The late Mopule Shadrack Montshiwagae

**For:** His encouragement and constructive guidance throughout my life and his emphasis on the importance of education.

# TABLE OF CONTENTS

|                          |   |            |
|--------------------------|---|------------|
| <b>DECLARATION</b>       |   | <b>ii</b>  |
| <b>ABSTRACT</b>          |   | <b>iii</b> |
| <b>ACKNOWLEDGEMENTS</b>  |   | <b>v</b>   |
| <b>DEDICATION</b>        |   | <b>vi</b>  |
| <b>GLOSSARY</b>          |   | <b>xi</b>  |
| <b>INTRODUCTION</b>      |   | <b>1</b>   |
| <b>CHAPTER 1</b>         |   |            |
| <b>PLANT BACKGROUND</b>  |   |            |
| <b>1.1</b>               | <b>General description of a PWR plant</b>             | <b>4</b>   |
| 1.1.1                    | Primary loop  | 4          |
| 1.1.2                    | Secondary loop  | 5          |
| 1.1.3                    | Tertiary loop   | 6          |
| <b>1.2</b>               | <b>Steam-water cycle description</b>                  | <b>6</b>   |
| 1.2.1                    | Single-phase (liquid)                                 | 7          |
| 1.2.2                    | Single phase (steam)                                  | 8          |
| 1.2.3                    | Two phases (liquid/steam)                             | 9          |
| <b>1.3</b>               | <b>Sampling system</b>                                | <b>10</b>  |
| <b>1.4</b>               | <b>Construction materials</b>                         | <b>13</b>  |
| <b>1.5</b>               | <b>Corrosion mechanisms</b>                           | <b>15</b>  |
| 1.5.1                    | Wastage, grooving, and stress corrosion cracking      | 15         |
| 1.5.2                    | Denting   | 15         |
| 1.5.3                    | Pitting   | 15         |
| 1.5.4                    | Flow accelerated corrosion                            | 16         |
| <b>1.6</b>               | <b>System chemistry</b>                               | <b>16</b>  |
| 1.6.1                    | Hydrazine application (single phase FAC)              | 20         |
| 1.6.2                    | Ammonia and ethanolamine application (two-phases FAC) | 22         |
| 1.6.3                    | Effect of impurities on FAC/corrosion products        | 25         |
| <b>CHAPTER 2</b>         |   |            |
| <b>RESEARCH OVERVIEW</b> |   |            |
| <b>2.1</b>               | <b>Research problem statement</b>                     | <b>28</b>  |
| <b>2.2</b>               | <b>Research questions</b>                             | <b>28</b>  |
| <b>2.3</b>               | <b>Research aims and objectives</b>                   | <b>28</b>  |
| <b>2.4</b>               | <b>Research hypothesis</b>                            | <b>29</b>  |
| <b>2.5</b>               | <b>Research scope and delimitation</b>                | <b>29</b>  |
| <b>2.6</b>               | <b>Research method</b>                                | <b>30</b>  |
| 2.6.1                    | Literature review                                     | 30         |
| 2.6.2                    | Data collection                                       | 30         |
| 2.6.3                    | Sample treatment                                      | 31         |
| 2.6.4                    | Sample analysis                                       | 31         |
| 2.6.5                    | Data treatment and statistics                         | 32         |

|   |   |    |
|---|---|----|
| <b>CHAPTER 3</b>                                      |   |    |
| <b>LITERATURE REVIEW</b>                              |   |    |
| <b>CHAPTER 4</b>                                      |   |    |
| <b>EXPERIMENTAL</b>                                   |   |    |
| 4.1   | Apparatus   | 40 |
| 4.2   | Reagents  | 40 |
| 4.3   | Instrumentation   | 40 |
| 4.4   | Placing of filters  | 40 |
| 4.5   | Retrieval of filters  | 41 |
| 4.6   | Digestion of filters  | 41 |
| 4.7   | Sample analysis   | 42 |
| 4.7.1   | Flame setup   | 43 |
| 4.7.2   | Analysis  | 43 |
| <b>CHAPTER 5</b>                                      |   |    |
| <b>RESULTS AND DISCUSSION</b>                         |   |    |
| 5.1   | Raw data for reactor power less than 30 %                   | 44 |
| 5.2   | Pictures of filter samples                                  | 45 |
| 5.3   | Graphical representation of data and sample filter pictures | 46 |
| 5.4   | Transport calculations                                      | 47 |
| <b>CHAPTER 6</b>                                      |   |    |
| <b>DATA TREATMENT</b>                                 |   |    |
| 6.1   | Data treatment and statistics                               | 51 |
| <b>CHAPTER 7</b>                                      |   |    |
| 7.1   | Conclusions   | 57 |
| 7.2   | Future work   | 59 |
| <b>REFERENCES</b>                                     |   | 60 |
| <b>APPENDICES</b>                                     |   |    |
| Appendix A: Recommended conditions for flame analysis |   | 63 |



## LIST OF FIGURES

|   |           |
|---|-----------|
| <b>Figure 1.1: Schematic diagram for Koeberg energy cycle</b>   | <b>4</b>  |
| <b>Figure 1.2: Steam/water cycle</b>  | <b>7</b>  |
| <b>Figure 1.3: Steam/water cycle heating curve</b>  | <b>9</b>  |
| <b>Figure 1.4: Steam/water cycle drains diagram</b>   | <b>10</b> |
| <b>Figure 1.5: Schematic diagram of a continuous sampling system</b>  | <b>11</b> |
| <b>Figure 1.6: NWT Model 100-B2 corrosion product sampler supplied by the NWT manufacturing corporation in California</b> | <b>12</b> |
| <b>Figure 1.7: Close-up of filter housing</b>   | <b>12</b> |
| <b>Figure 1.8: The blast furnace</b>  | <b>14</b> |
| <b>Figure 1.9: A general schematic diagram of corrosion films</b>   | <b>17</b> |
| <b>Figure 1.10: Schematic diagram depicting flow-accelerated corrosion</b>  | <b>19</b> |
| <b>Figure 1.11: The effect of hydrazine on oxidation-reduction potential and iron concentration</b>                       | <b>20</b> |
| <b>Figure 1.12: Solubility of magnetite as a function of temperature at various ammonia concentrations</b>                | <b>22</b> |
| <b>Figure 1.13: Effect of pH on corrosion rate of carbon steel in two chemicals at 150 °C</b>                             | <b>24</b> |
| <b>Figure 1.14: Effect of temperature on corrosion rate of carbon steel in two different chemicals at pH 9.5</b>          | <b>24</b> |
| <b>Figure 3.1: Total mass of steam generator sludge per fuel cycle</b>  | <b>34</b> |
| <b>Figure 3.2: Schematic of vertical PWR steam generator</b>  | <b>37</b> |
| <b>Figure 3.3: Sludge build up on tube support plate and on the tubes</b>   | <b>37</b> |
| <b>Figure 4.1: Corrosion product sampler flow diagram</b>   | <b>41</b> |
| <b>Figure 4.2: Picture of Perkin Elmer 7000 atomic absorption spectrophotometer</b>                                       | <b>42</b> |
| <b>Figure 5.1: Pictures of AHP 2 filter samples</b>   | <b>45</b> |
| <b>Figure 5.2: Pictures of 2CEX filter samples</b>  | <b>45</b> |
| <b>Figure 5.3: Graphical representation of particulate vs. soluble iron concentrations for AHP2</b>                       | <b>46</b> |
| <b>Figure 5.4: Graphical representation of particulate vs. soluble iron concentrations for 2CEX</b>                       | <b>47</b> |
| <b>Figure 6.1: Curve of cumulative iron amounts</b>   | <b>52</b> |

## LIST OF TABLES

|   |           |
|---|-----------|
| <b>Table 1.1: Temperature profile across the feed heaters</b>   | <b>8</b>  |
| <b>Table 1.2: Eight forms of iron oxides and oxyhydroxides</b>  | <b>26</b> |
| <b>Table 2.1: Template for sample results</b>   | <b>31</b> |
| <b>Table 3.1: EPRI Survey Results</b>   | <b>34</b> |
| <b>Table 3.2: Elemental analysis of sludge sample</b>   | <b>35</b> |
| <b>Table 3.3: Mossbauer spectral components for sludge sample at room temperature</b>                               | <b>36</b> |
| <b>Table 5.1: AHP2 and 2CEX iron concentration results</b>  | <b>44</b> |
| <b>Table 5.2: Transport amounts as calculated for less than 30 % reactor power and 11 days basis of up to 100 %</b> | <b>48</b> |
| <b>Table 5.3: AHP2 Iron data for 100 % reactor power and the whole fuel cycle</b>                                   | <b>50</b> |
| <b>Table 6.1: Tabulation of cumulative amounts and inputs into the regression expression</b>                        | <b>51</b> |
| <b>Table 6.2: Tabulation of inputs into the standard error expression</b>   | <b>55</b> |

## GLOSSARY

| <b>Terms/Acronyms / Abbreviations</b> | <b>Definitions/Explanation</b>          |
|---------------------------------------|---|
| ACO                                   | Feedwater heater drains recovery system |
| AHP                                   | Feedwater heating system                |
| APP                                   | Main feedwater pumps system             |
| ASG                                   | Auxiliary water supply system           |
| CEX                                   | Condenser extraction system             |
| DLS                                   | Diamond light sources                   |
| EDF                                   | Electric de France                      |
| EPRI                                  | Electric Power Research Institute       |
| ETA                                   | Ethanolamine                            |
| GSS                                   | Moisture separator re-heater system     |
| PWR                                   | Pressurised water reactor               |
| WANO                                  | World Association of Nuclear Operators  |
| EDF                                   | Electric de France                      |



## INTRODUCTION

The beginning of commercial operation of Koeberg Nuclear Power Station (KNPS) in 1984 and 1985 for both Unit 1 and Unit 2 respectively was not without any chemistry related challenges with respect to general material integrity in terms of corrosion product formation, transportation and deposition into the steam generators.

Corrosion products in the power generating industry are directly related to flow accelerated corrosion (FAC) phenomenon which is experienced extensively in the fossil power plants and is related to material loss and corrosion product transport into the steam generators. An example of the extent of the problem that can arise as a result of FAC is when in 1986 December 09 at Surry Nuclear Power Station an elbow in the condensate system (CEX) ruptured, causing four fatalities and tens of millions of dollars in repair costs and lost revenue and FAC was found to be the cause of the failure.

In addition, corrosion products in the feedwater are transported and deposited into the steam generators thereby causing steam generator tube fouling, which affects the heat transfer characteristics of the tubes and provide areas for impurity accumulation. This can in turn alter the chemistry of the local environment and lead to various corrosion mechanisms that can affect material integrity of the tubes. In the nuclear industry, this is particularly undesirable because the tubes are the most sensitive part of the nuclear power plant in terms of nuclear safety.

But given that the concentration of corrosion products during normal operation across the nuclear industry has reduced over the years owing to the application of various amine technologies and other factors, the focus has now shifted more towards the need to reduce corrosion product transport during a startup phase. Therefore, the focus of this work will be around corrosion product transport during startup and its contribution to the total fuel cycle transport amount.

Chapter one of this research study gives a plant background, followed by a detailed description of the steam/water cycle to describe the feedwater, steam and water/steam circuits. This is complemented by outlining the sampling system, its limitations and possible errors that would arise due to design features and how these are overcome. The different corrosion mechanisms are also highlighted with brief explanations and a detailed focus on flow accelerated corrosion mechanism as it forms the basis for system chemistry.

A detailed description and explanation of system chemistry and how it leads to the type of oxide formed on metal surfaces under a different set of physical conditions of temperature and thermal hydraulics is presented. One of the key factors in determining the applied chemistry regime and type of resultant corrosion products is the materials of construction and as such, a background to construction materials of the steam/water circuit is given.

To reduce corrosion products in the feedwater and water/steam circuits, a chemistry regime in which both an amine (for pH control) and a reducing agent (for control of redox conditions) are added into the feedwater is applied. Chapter one concludes by discussing the various types of feedwater treatment methods with explanations about which method is applied for which part of the steam/water circuit, such as hydrazine application for single phase feedwater side and a consideration of the effects of impurities on FAC, particularly how these impurities affect corrosion rates and oxide morphology.

Chapter two states the research problem, research questions, research aims and objectives, the hypothesis and scope and delimitation. A full outline of the research approach adopted in the research process including data collection, sample treatment and transport calculations is also given under chapter two. Literature review is covered under chapter three and was carried out to gain insight into what has been done across industry with respect to evaluation of corrosion products during startup. The indication is that there is no consistent data as the results differ from one plant to the other and from one startup to the next.

Corrosion products are also of concern in the different industries, in the water industry they affect water quality and result in high energy demands for water delivery along the pipes due to scale formation on the internal surface of water delivery pipes. In the accelerator industry, corrosion products affect reliability and operation given that particulate copper oxide clogs control valves and cooling water components resulting in unplanned shutdowns. Thirdly, highlight is made of the transport industry where corrosion products lead to cracks and structural degradation, thereby leading to costly civil maintenance interventions to restore structural integrity to concrete structures. Lastly, in the archaeological and artistic work, the problem highlighted about corrosion products is that of preservation. This makes it necessary that the artefact be conserved and depending on the type and extent of corrosion product formation on the surface, the effectiveness of restoration might be affected. A brief overview of the phenomenon of steam generator fouling and hideout and how they relate to corrosion product was also given, with a brief account of the origins of steam generator sludge composition and its elemental constituents.

Experimental work is covered under chapter four in which the sampling procedures of placing, retrieving and digestion of sample filters are outlined, this includes sample analysis procedures. Results are presented in chapter five accompanied by a discussion of relevant and important points. Lastly, chapter six lists all the conclusions as they relate to the research objectives.

# CHAPTER 1

## PLANT BACKGROUND

### 1.1 General description of a PWR plant

Figure 1.1 is a simplified schematic diagram depicting a general overview of the energy cycle of a typical PWR nuclear power plant. A PWR power plant consists of three heat transfer loops, namely, the primary loop, secondary loop and tertiary loop.

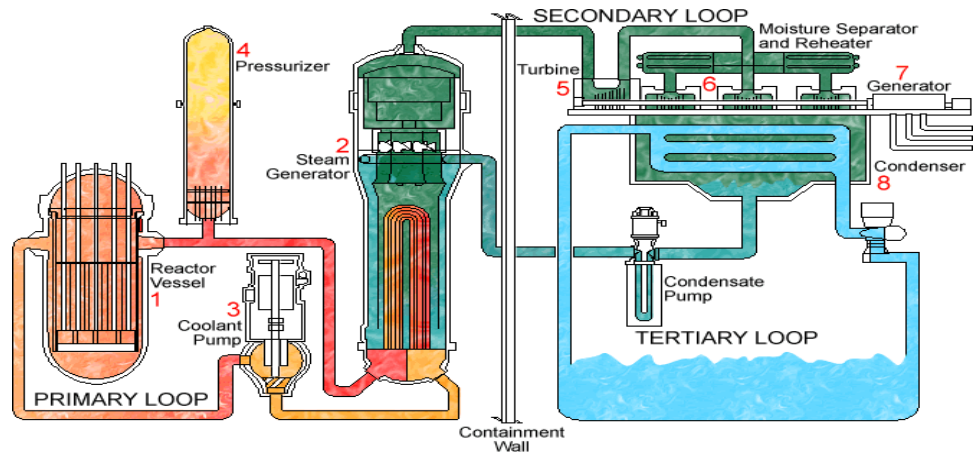


Figure 1.1: Schematic diagram for Koeberg energy cycle

(Adopted from [www.eskom.co.za/aboutelectrocity/visitorcenters/pages/koeberg\\_power\\_station.aspx](http://www.eskom.co.za/aboutelectrocity/visitorcenters/pages/koeberg_power_station.aspx))

[36]

#### 1.1.1 Primary loop

The primary loop consists of a reactor vessel, reactor coolant pumps, steam generator tubes, the pressuriser and the reactor coolant.

- Reactor vessel

The reactor vessel houses the reactor core made-up of fuel assemblies composed of individual fuel rods. The source of energy/fuel in a PWR reactor is typically uranium enriched in  $U^{235}$  atoms. A PWR reactor is governed by the interaction of neutrons with the nucleus of uranium atoms and takes advantage of the concept of mass defect related to the total binding energy liberated in a fission reaction and is used to heat-up the water [4].

- Reactor coolant

The coolant, boric acid ( $H_3BO_3$ ) containing water in this case, is mainly used to cool the reactor core and to moderate the nuclear fission reaction. Boric acid acts as a chemical shim meant to arrest neutron leakage from the reactor core to prevent power spikes which are not desirable from a nuclear reactor safety point of view. [4].



- Reactor coolant pumps

Reactor coolant pumps are used to pump the pressurised coolant across the reactor core to pick up the heat and to transfer this heat to the steam generators in order to evacuate the heat.

- Pressuriser

Given the amount of heat output of a fission reaction, the water coolant temperature exceeds its boiling point and would boil at atmospheric pressures. Therefore, the pressuriser prevents the coolant from boiling by maintaining relatively high operating pressures of about 15 MPa at  $> 300\text{ }^{\circ}\text{C}$ .

- Steam generator (tubes)

The steam generator performs a cooling function by acting as a heat sink by exchanging the heat content of the reactor coolant with the secondary fluid in contact with the steam generator tubes. The steam generator tubes also act as a barrier between the primary (radioactive) loop side and the conventional side to prevent contact between the fluids of both loops.

#### 1.1.2 Secondary loop

The function of the secondary loop is to act as a coolant for the steam generators and consists of the feed heaters, condenser, steam generators, steam turbines and feed pumps.

- Feed trains

The feed trains in the secondary loop consists of low and high-pressure heaters with the interconnecting pipe work, the heaters are used to preheat the feedwater before entering the steam generators to ensure efficient heat transfer in the steam generators. The feedwater is heated to about  $286\text{ }^{\circ}\text{C}$  at a discharge pressure of the last feed pumps before the steam generators.

- Steam Generators

The steam generators serve to produce steam of a required quality in terms of the moisture content for use in the high-pressure steam turbine.

- Steam turbines

The steam turbines convert the heat energy in the steam to mechanical energy which in turn is converted to electrical energy by turning in a magnetic field to produce electricity.

- Condenser

The condenser is used to collect the exhaust condensate resulting from the low-pressure steam turbines following its loss of energy after doing work in the turbines.

- Feedwater pumps

Feedwater pumps are used to extract the condensate from the condenser and to pump it into the feed trains and up to the steam generators.

### 1.1.3 Tertiary loop

The conversion efficiency of the total amount of heat energy output of the reactor to electrical energy is reported to be just over 30 %, the rest of the heat must be rejected, and this is done via the condenser into the tertiary loop of the plant.

## 1.2 **Steam-water cycle description**

The production of electric energy through the steam/water cycle occurs by a series of thermodynamic transformations and as such, the function of a thermodynamic power cycle is to convert heat energy into work [5]. The cycle can be split into three sections, single liquid phase, single steam phase and steam/water mixture. The steam phase section is generally thought to not experience FAC and corrosion problems as compared to the other two sections owing to its low moisture content.

### 1.2.1 Single-phase (liquid)

Figure 1.2 below is a skeleton diagram depicting Koeberg's steam/water cycle on which a detailed description will be based:

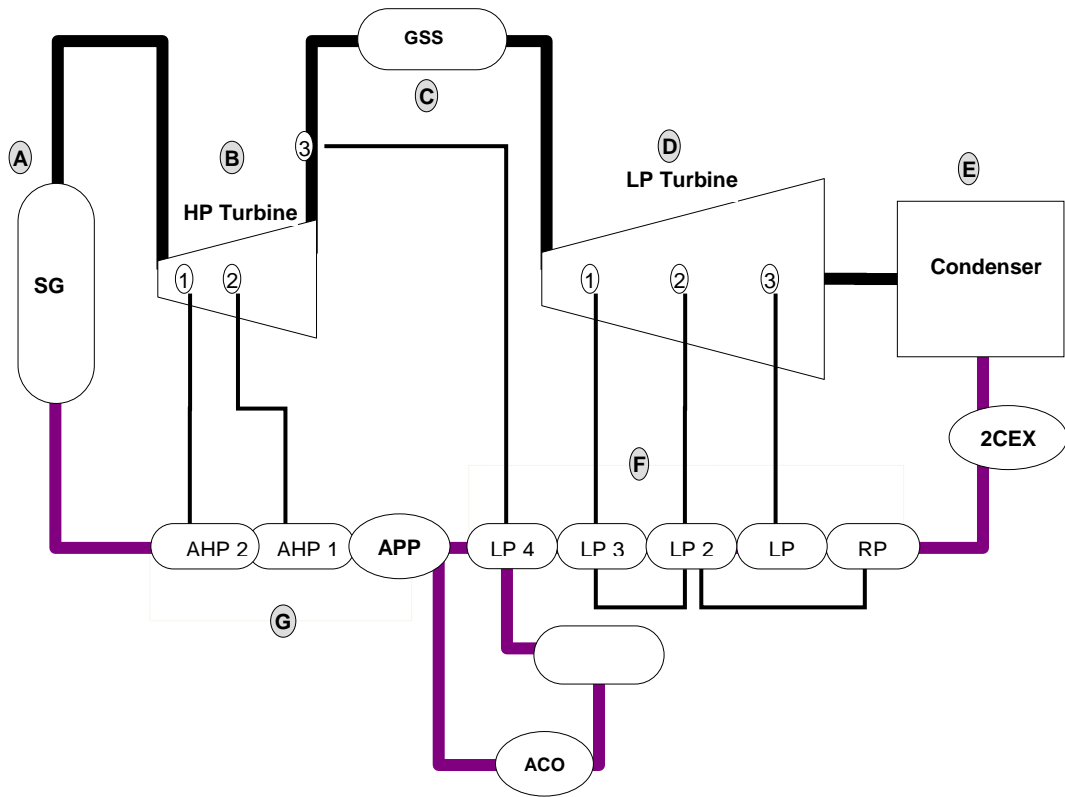


Figure 1.2: Steam/water cycle

(Adapted from Feed Train Layout Detail. Koeberg Training Presentation) [3]

In the above diagram from the portion labelled 2CEX coming from the condenser up to RP1 (drains cooler heater), the water/condensate is pumped by the condensate extraction pumps (CEX) to a point labelled APP. The water temperature from the condenser is 31 °C at 4.5 MPa discharge pressure of the pumps, the condensate is then gradually heated up through a series of feedwater heaters. The first set of heaters is the drains cooler heater (RP1) which heats up the water to 35 °C. The temperature profile from section F represented by RP1 to LP4 (low pressure heater) up to section G represented by AHP1 (high pressure heater) to AHP2 in the diagram is reflected in Table 1.1:

**Table 1.1: Temperature profile across the feed heaters**

| Section F | Inlet temperature °C | Outlet temperature °C | $\Delta T$ °C | Section G | Inlet temperature °C | Outlet temperature °C | $\Delta T$ °C |
|-----------|----------------------|-----------------------|---------------|-----------|----------------------|-----------------------|---------------|
| RP1       | 31                   | 35                    | 4             | AHP1      | 182                  | 200                   | 18            |
| LP1       | 35                   | 56                    | 21            | AHP2      | 200                  | 220                   | 20            |
| LP2       | 56                   | 93                    | 37            |           |                      |                       |               |
| LP3       | 93                   | 134                   | 41            |           |                      |                       |               |
| LP4       | 134                  | 180                   | 46            |           |                      |                       |               |

When the water exits AHP2 in section G, its temperature is 220 °C at 7 MPa discharge pressure of the APP feedwater pumps and it is now referred to as feedwater because it is ready to be injected into the steam generators [3]. Up to this point, the whole section represents a single-phase region of the steam/water circuit.

### 1.2.2 Single phase (steam)

In the steam generators (SG) or section A in Figure 1.2, the feed water flows downwards and then upwards through the steam generator tubes and picks up heat energy from the hot primary coolant flowing through the tubes. It is within the steam generators that the feedwater undergoes phase-transition from liquid to gas or steam, because the steam originates from boiling of water, it becomes saturated steam containing some degree of moisture at equilibrium. During a phase transition period water absorbs large amounts of heat energy and it is this energy in addition to the one added during heating of water from RP1 that is converted to electric energy [5].

In section B, the steam is used to drive the high-pressure steam turbine to convert heat energy into mechanical energy and as such performances work and losses some of its energy with an accompanied increase in the moisture content that would otherwise pose corrosion problems in the low-pressure steam turbines in section D. To prevent this moisture from reaching the low-pressure turbines, the steam is then directed from the HP turbine (section B) to the moisture separator re-heaters in section C labelled GSS, here the moisture is removed and the steam superheated from which it is directed to the low-pressure steam turbines in section D. Once the steam has done work in these last set of steam turbines, it then exhausts into the condenser in which excess amount of heat energy is rejected into the cooling tertiary loop and the steam is condensed back to the liquid phase [5]. This part represents the steam circuit of the steam/water cycle. Figure 1.3 is a heating curve of the steam/water cycle situation as it occurs from F to E:

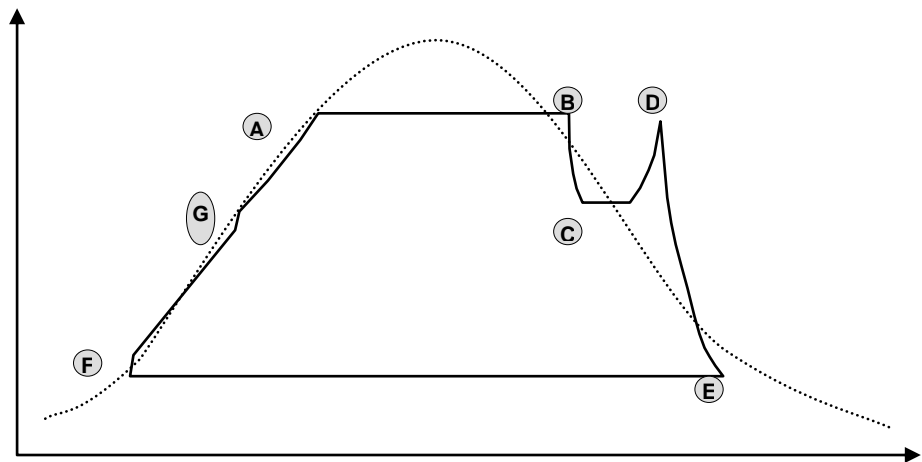


**Figure 1.3: Steam/water cycle heating curve**

**(Adapted from Feed Train Layout Detail. Koeberg Training Presentation) [3]**

In section A, phase-transition from the liquid to gaseous state occurs at a constant temperature while at section B the steam performs work in the high-pressure turbine resulting in a temperature drop to C in the curve. A temperature increase from section C to section D represents superheating of the steam before entering section D where it performs further work in the low-pressure turbines and losses some of the energy with further loss of the excess amount of energy in section D dropping the temperature back to 31 °C.

### 1.2.3 Two phase (liquid/steam)

The numbers 1 – 8 in Figure 1.4 indicates the locations from which the heating steam for LP4, AHP1 and AHP2 feed heaters is tapped-off, numbers 9 – 11 indicates the heating steam source for LP1, LP2 and LP3 feed heaters. The heating steam for GSS is tapped-off from the steam coming directly from the steam generators (SG). Once the steam has performed its heating function, it drains from LP4, AHP1, AHP2 and GSS cascades to the heater drains tank labelled ACO as a mixture of steam and water. The only drains that returns to the condenser are those from RP1, LP1, LP2 and LP3, also forming a two-phase (steam/water) mixture.

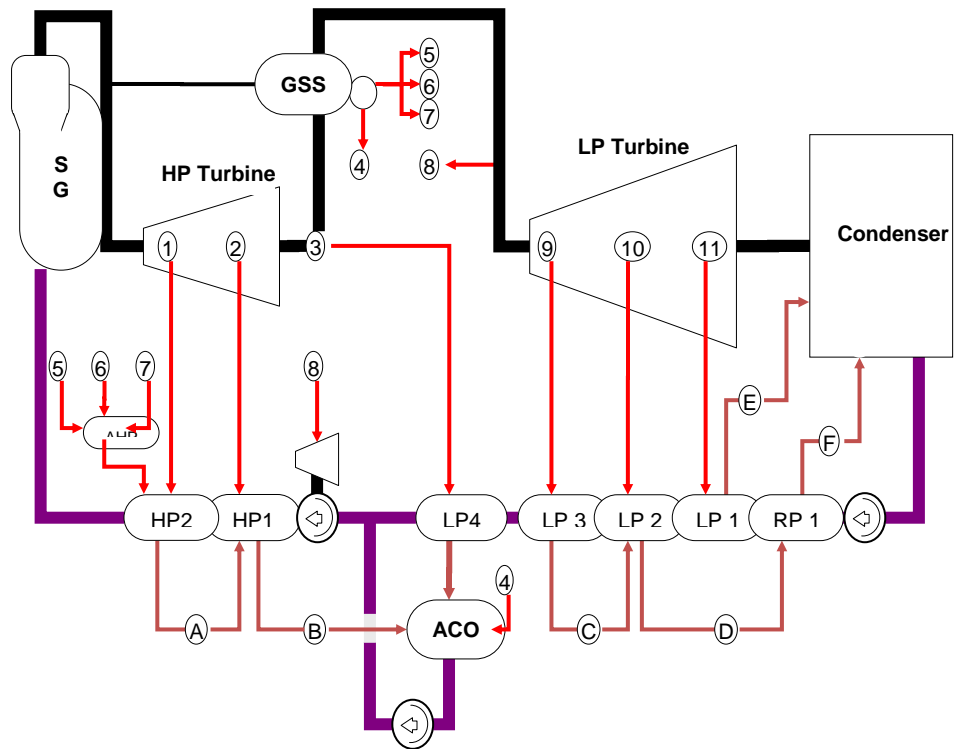


**Figure 1.4: Steam/water cycle drains diagram**

(Adapted from Feed Train Layout Detail. Koeberg Training Presentation) [3]

### 1.3 Sampling system

In terms of the requirements for correct operation and proper conservation of the Koeberg plant, the liquid chemical characteristics of the secondary water/steam circuit together with its support systems must comply with prescribed specifications. To determine these liquid characteristics, a sampling system was installed to collect samples for this purpose. Chemical characteristics include corrosion products, hydrazine ( $N_2H_4$ ), dissolved oxygen ( $O_2$ ) and pH amongst others.

Two types of sampling are established, namely, continuous and manual sampling. With continuous sampling a sample is drawn from a relevant system's sampling point and routed via coolers to the sampling rooms where it can be cooled further to the required temperature for the analysers to function properly and to provide accurate readings. The sample lines are installed with pressure control valves to reduce pressure of the sample line to a pressure low enough for fragile equipment.

For manual sampling, samples can be drawn from various system sample points and sampled using portable in-line analysers or can be removed to the chemistry laboratory for manual analysis [7]. A typical sampling line is as depicted in Figure 1.5:

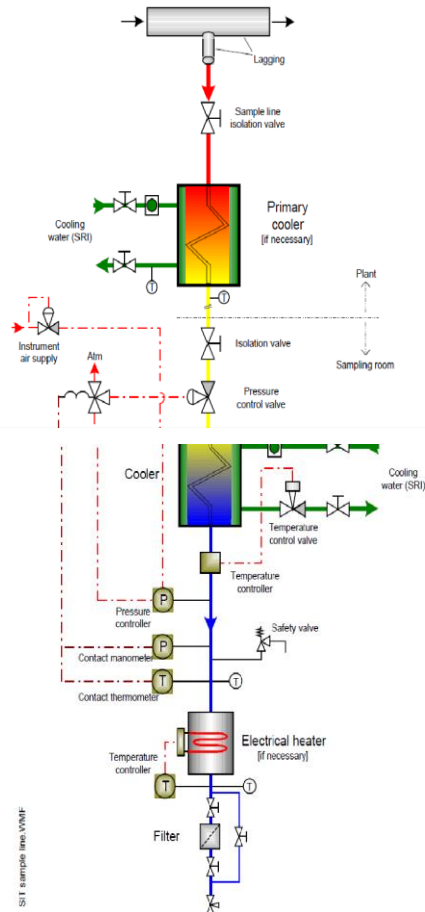


**Figure 1.5: Schematic diagram of a continuous sampling system**

**(Adapted from Comper, J.D, 2003:7) [7]**

However, sample line designs like those for AHP2 and 2CEX are such that they are lengthy from their respective systems to the sample point. Other sample line features include root isolation valves, bends, high and low temperature coolers, orifices, manually controlled isolation valves, drain valves and pressure control valves.

Therefore, these design features would introduce errors or underestimation in particulate determination of corrosion products due to particle dropouts. Also, because of the low levels of corrosion products during steady state plant operation, manual sampling would not be adequate and representative.

To circumvent these difficulties, Koeberg has installed the NWT integrating sampler at strategic locations closer to the origin of the sample lines. In Figure 2.2, the integrating samplers are installed downstream of AHP2 (No.6 feedheater), downstream ACO and downstream 2CEX. The NWT sampler is depicted in Figure 1.6:

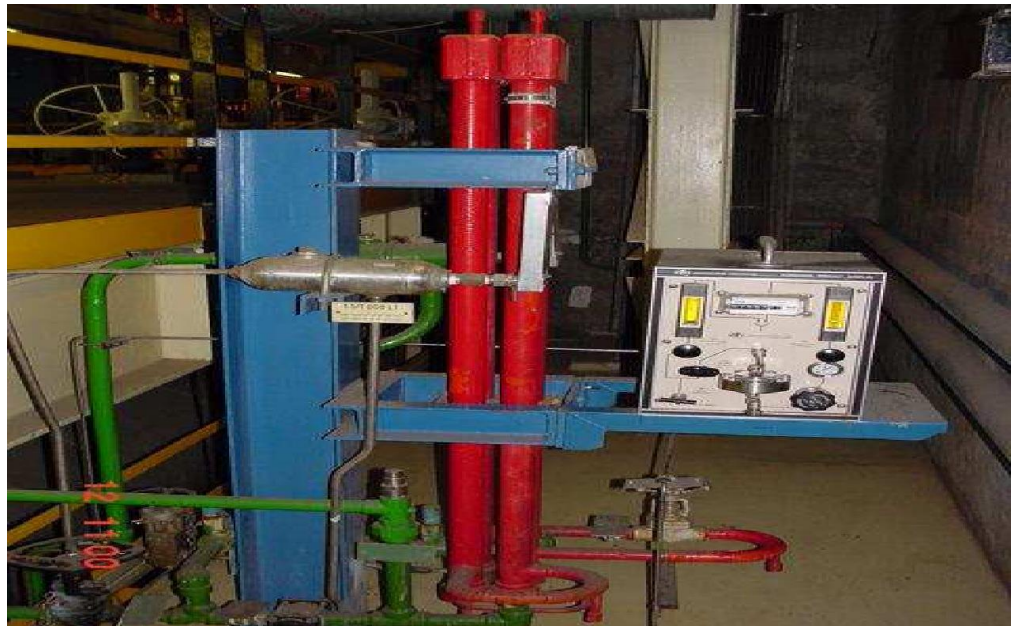


Figure 1.6: NWT Model 100-B2 corrosion product sampler supplied by the NWT manufacturing corporation in California

(Adapted from Eeden, N & Galt, K.J, 2006:3) [10]

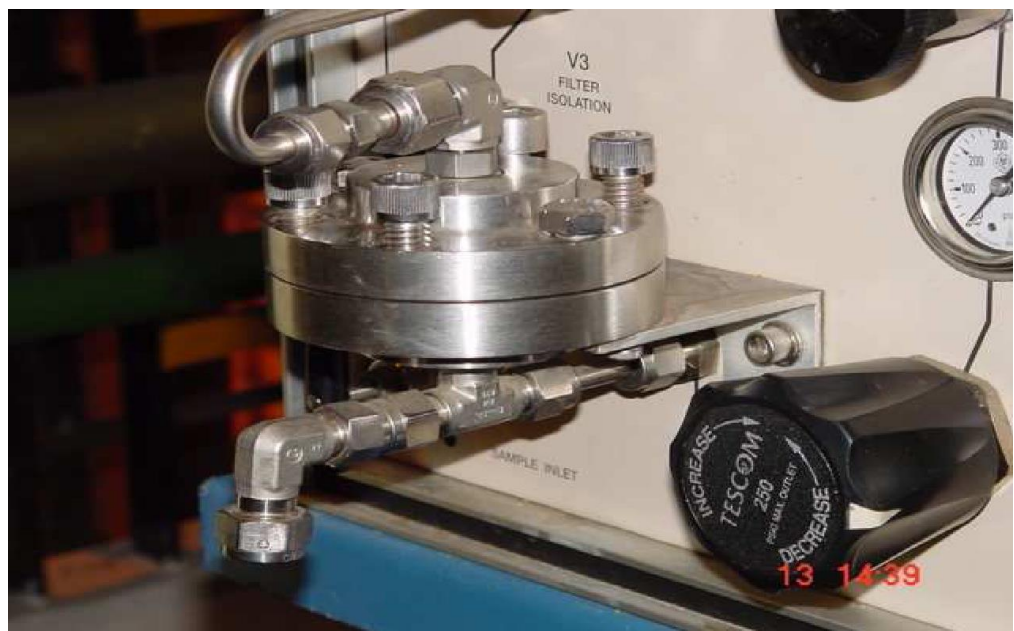


Figure 1.7: Close-up of filter housing

(Adapted from Eeden, N & Galt, K.J, 2006:3) [10]



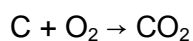
The advantages of this sampling equipment are that it operates at system pressure thereby eliminating the need for pressure reduction, it assures high sample line velocity and turbulence level with minimal variations in the sample line flowrate during membrane packet change-outs [11]. All these factors minimize particulate dropouts and enhances corrosion product determination accuracy.

With this technique, the solid material is accumulated on a filter paper and the dissolved metal ions are simultaneously collected on successive cation resin-impregnated filter papers. The solid and dissolved materials are then separated, digested with acids and analysed to determine the insoluble and soluble concentrations [10]. The sampling comprises of flushing the sample line for systems that are not in continuous sampling mode, placing of filters and retrieval of filters after a predetermined period.

#### **1.4 Construction materials**

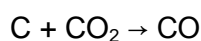
Construction material is one of the key factors considered for the type of chemistry to be applied in a nuclear power plant. The type of construction materials being selected will determine how it will react to the applied chemistry regime under various set of thermal-hydraulic conditions, it will determine the reaction rates and type of corrosion products. Koeberg's steam/water circuit has its major components constructed mainly from carbon and stainless steel and as such, it is generally referred to as all-ferrous.

Various types of steels are produced by extracting iron (Fe) from its mined ores, the most common ores are haematite ( $\text{Fe}_2\text{O}_3$ ) and magnetite ( $\text{Fe}_3\text{O}_4$ ). The extraction steps include burning coke (produced by heating coal in the absence of air) in the blast of hot air to form carbon dioxide ( $\text{CO}_2$ ):



##### **Equation 1.1**

Carbon dioxide reacts with carbon at high temperature at the bottom of the furnace to produce carbon monoxide (CO)



##### **Equation 1.2**

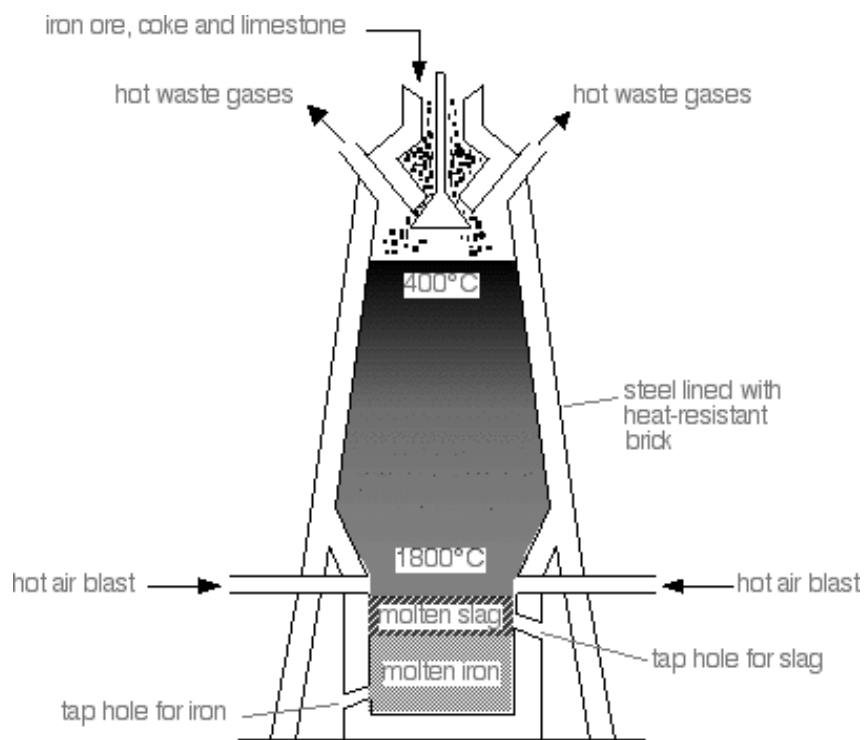
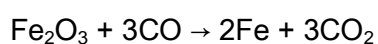


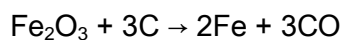
**Figure 1.8: The blast furnace**

(Adapted from <http://www.chemguide.co.uk/inorganic/extraction/iron.html>) [20]

The carbon monoxide (CO) then reacts with hematite ( $\text{Fe}_2\text{O}_3$ ) to reduce it to iron (Fe), and the carbon itself also acts as a reducing agent by reducing hematite ( $\text{Fe}_2\text{O}_3$ ) further and the respective reactions are as follows:



**Equation 1.3**



**Equation 1.4**

The reduced iron is then collected at the bottom of the furnace as molten iron which contains various impurities such as assortment of rocky material that contains silicon dioxide ( $\text{SiO}_2$ ). Other impurities include sulphur, carbon, phosphorus, and silicon which must be removed if the molten iron is to be used to produce various types of steels or alloys. Examples include mild steel, which is iron containing up to almost 0.25 % of carbon and high carbon steel containing up to about 1.5 % of carbon.

These iron products contain iron in the reduced redox state (Fe), whereas the iron ore itself contains iron in an oxidized redox state ( $\text{Fe}^{3+}/\text{Fe}^{2+}$ ) in combination with environmental oxygen ( $\text{O}_2$ ). This implies that iron in carbon/mild steel will be reactive to its environment as it attempts to return to its natural state. Therefore, the various steel types are simply produced by varying the percent carbon and chrome content or for strength and other properties by varying any other element in the final molten iron. The construction material for Koeberg's steam/water circuit being considered "all-ferrous" ranges in the 0.25 % carbon, with the replacement components ranging from 1 – 2 % Cr content [20].

The non-ferrous materials are the steam generator tubes made of nickel alloy (Inconel 600) and the titanium condenser tubes. The balance of plant is mainly constructed from copper (Cu), such as the turbine gland steam condenser, the condensers of vacuum pumps and impellers of the extraction pumps, piping of pressure gauges, valve seats/facings and pump bearings [10].

## 1.5 Corrosion mechanisms

Literature defines corrosion in many ways, but according to the corrosion and wear handbook for water cooled reactors, corrosion is defined as any process that involves the transfer of atoms from metallic to the ionic state. It further states that all dissolution and scale formation reactions come under this definition [9].

### 1.5.1 Wastage, grooving, and stress corrosion cracking

This mechanism is encountered in the condenser where air extraction from the steam space and consequent airflow causes a relatively higher concentration of oxygen ( $\text{O}_2$ ) within air extraction areas. The tubes nearest to the centre of the bundle receiving little steam with normal cooling creates the cold spots where incondensable gases such as ammonia ( $\text{NH}_3$ ) will collect. Localized flow can create deep circumferential grooves in the tube immediately next to the support plate if the condensate contains high levels of ammonia and oxygen [13].

### 1.5.2 Denting

Growing layers of oxides in the tube support plate holes do not seal the metal and allow chlorides to attack the metal; these oxides occupy a higher volume than the base metal and hence dent the tubes, leading to an increase of stress. This results in the occurrence of longitudinal cracking of the tubes and in the longer term to primary to secondary leaks [13].

### 1.5.3 Pitting

This corrosion occurs during normal operation on Inconel 600 tubes and is exacerbated by the presence of sulphur or copper compounds. Copper accounted for the majority of cases

where this mechanism has occurred, it also occurs when oxidising agents such as oxygen or copper oxides are present in an acidic environment which is created by the presence of chlorides or sulphates [13].

#### 1.5.4 Flow accelerated corrosion (FAC)

FAC is said to be an extension of the generalized corrosion in stagnant water with the difference being the effect of flowing water at the oxide-solution interface. Furthermore, it involves the dissolving of protective oxide layer on carbon or low alloy steel into a stream of flowing water or a water/steam mixture, and because liquid water is necessary to remove the oxide from the surface, it does not occur in a dry or superheated steam flow. During this process, the oxide layer becomes thinner and less protective thereby increasing corrosion rates.

FAC is the predominant corrosion mechanism and degradation phenomenon encountered in the steam/water circuits of PWR's and fossil power plants, factors affecting it include construction material, hydrodynamic disturbances, system temperature and water chemistry [12].

### 1.6 System chemistry

The rationale behind the system water chemistry follows the mechanism involved in flow accelerated corrosion and the factors affecting it. FAC mechanism is based on the corrosion of iron in aqueous solution in which oxidation and reduction reactions occur at anodic and cathodic sites respectively as follows:



#### Equation 1.5

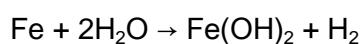


#### Equation 1.6



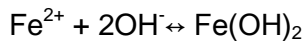
#### Equation 1.7

Combination of anodic and cathodic reactions gives the following overall reaction:



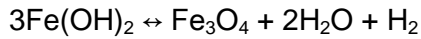
#### Equation 1.8

The ultimate equilibrium between ferrous hydroxide and iron ions is thus:

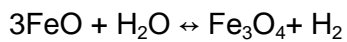


**Equation 1.9**

The ferrous hydroxide then decomposes into magnetite as follows according to Schikorr reactions:



**Equation 1.10**



**Equation 1.11**

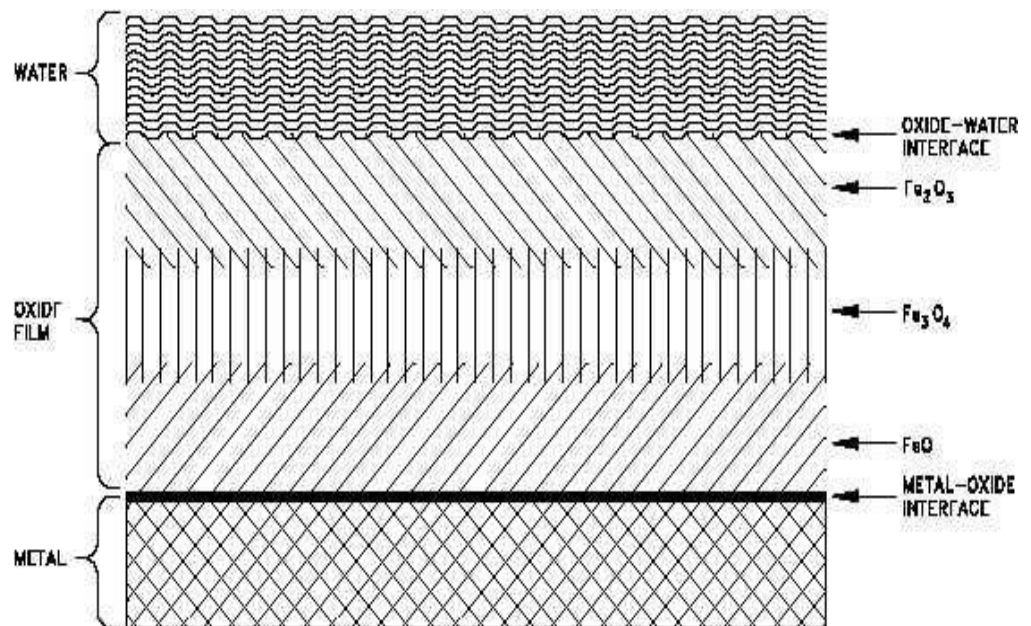
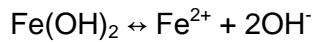


**Figure 1.9: A general schematic diagram of corrosion films**

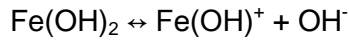
**(Adapted from Pressurized Water Reactor Primary Zinc Application Guidelines. EPRI, Palo Alto, CA: 2006. 1013420) [28]**

The magnetite thus formed on the surface of the metal (carbon steel) acts as a protective film that inhibits further corrosion of the base metal under a given set of conditions (alkaline reducing), therefore its stability is a function of the adjacent water chemistry. This magnetite is reportedly composed of topotactic and epitactic parts whereby a dense topotactic layer grows directly on the surface of the steel, while the more porous epitactic layer forms above

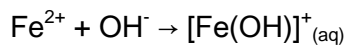
the topotactic layer [12]. The ferrous hydroxide decomposition reactions towards magnetite are as follows [31]:



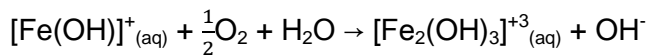
**Equation 1.11**



**Equation 1.12**

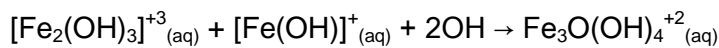


**Equation 1.13**, this reaction is followed by subsequent oxidation of soluble ferrous hydroxide form  $[\text{Fe(OH)}]^+_{(\text{aq})}$



**Equation 1.14**

The oxidized entity  $[\text{Fe}_2(\text{OH})_3]^{+3}_{(\text{aq})}$  can then react with another soluble ferrous hydroxide entity to form an entity which has the same  $\text{Fe}^{2+}/\text{Fe}^{3+}$  ratio as magnetite as follows:



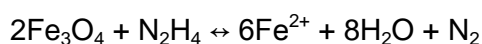
**Equation 1.15**

At high oxidation or low pH, further oxidation to goethite (or other  $\text{Fe}^{3+}$  oxyhydroxides) can happen. If the concentration of oxygen in the water is low and the pH is high, slow oxidation will take place resulting in dehydroxylation before oxidation such that the intermediate transfers to crystalline magnetite according to the following reaction [31]:



**Equation 1.16**

The dissolution-reduction reaction of magnetite at the oxide/water interface is as follows:



**Equation 1.17**

$\frac{1}{3}\text{Fe}_3\text{O}_4 + (2-b)\text{H}^+ + \frac{1}{3}\text{H}_2 \rightarrow \text{Fe}(\text{OH})^{(2-b)+} + (\frac{4}{3} - b)\text{H}_2\text{O}$  (only at temperature above 200 °C in the presence of hydrogen) b = 0, 1, 2, 3, 4

**Equation 1.18**

Therefore, FAC and corrosion process proceeds initially by steel oxidation at metal/oxide interface which leads to the production of soluble ferrous ions and magnetite, the soluble ion species diffuses through the oxide layer porosities from the metal surface to the main water flow. The hydrogen produced at the metal-oxide interface also diffuses into the water via the oxide porosities or through the steel. The magnetite then dissolves through a dissolution-reduction at the oxide-water interface accompanied by another diffusion of soluble ion species into the flowing water from the oxide/water interface and hydrogen transfer in air by convection. The consumption of soluble iron species at the oxide/water interface is the actual driving force for steel oxidation which in turn increases the corrosion process [12]. The process is depicted schematically in Figure 1.10.

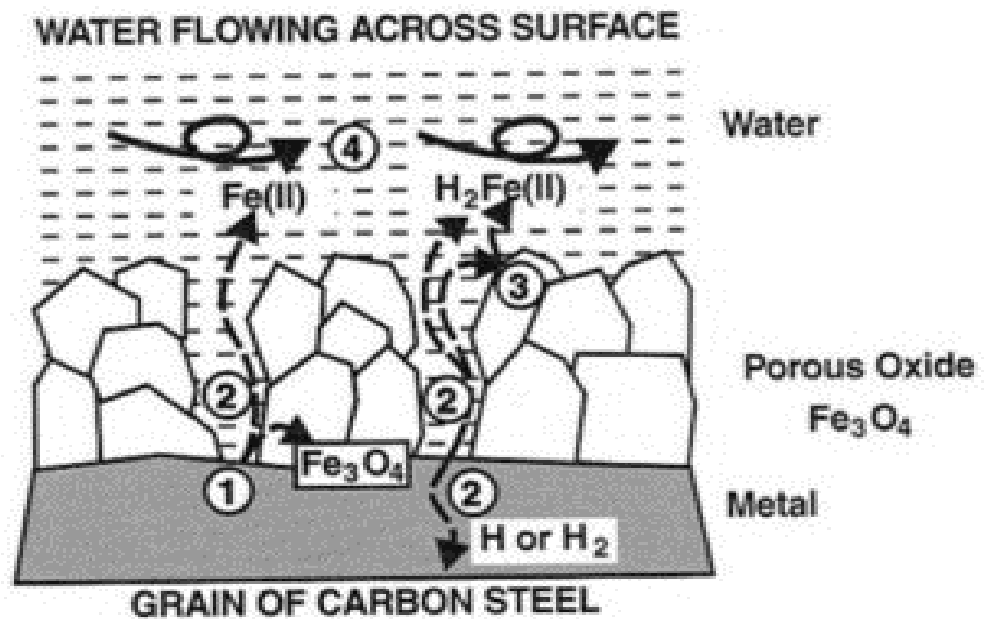


**Figure 1.10: Schematic diagram depicting flow-accelerated corrosion**

(Adopted from Rhee, H.et al., 2014:431) [30]

Currently there are three types of feedwater treatment methods that are applied across industry to mitigate FAC, namely, AVT(R) all volatile treatment with ammonia and a reducing agent, AVT(O) all volatile treatment with only ammonia addition, and OT which is oxygen treatment with ammonia and oxygen additions [14].

At Koeberg, AVT(R) with the addition of ammonia and hydrazine as a reducing agent is the applied feedwater treatment method. This option was selected over the other two given that PWR's with recirculating steam generators requires operation under reducing conditions to protect the Inconel 600 steam generator tubes from corrosion. Therefore, the water entering the steam generators must be deoxygenated to ensure a reducing environment. Most of the oxygen is removed through deaeration system in the condenser, good condenser vacuum with residual oxygen scavenged by the added hydrazine [1].

### 1.6.1 Hydrazine application (single phase FAC)

For a single-phase feedwater line conditioned with hydrazine for residual oxygen removal and reducing conditions as required for the steam generators, the predominant protective oxide layer will be magnetite ( $\text{Fe}_3\text{O}_4$ ). The overriding factor affecting corrosion and FAC will be the feedwater oxidizing-reducing potential (ORP) and the solubility of magnetite will be influenced by the reducing conditions.

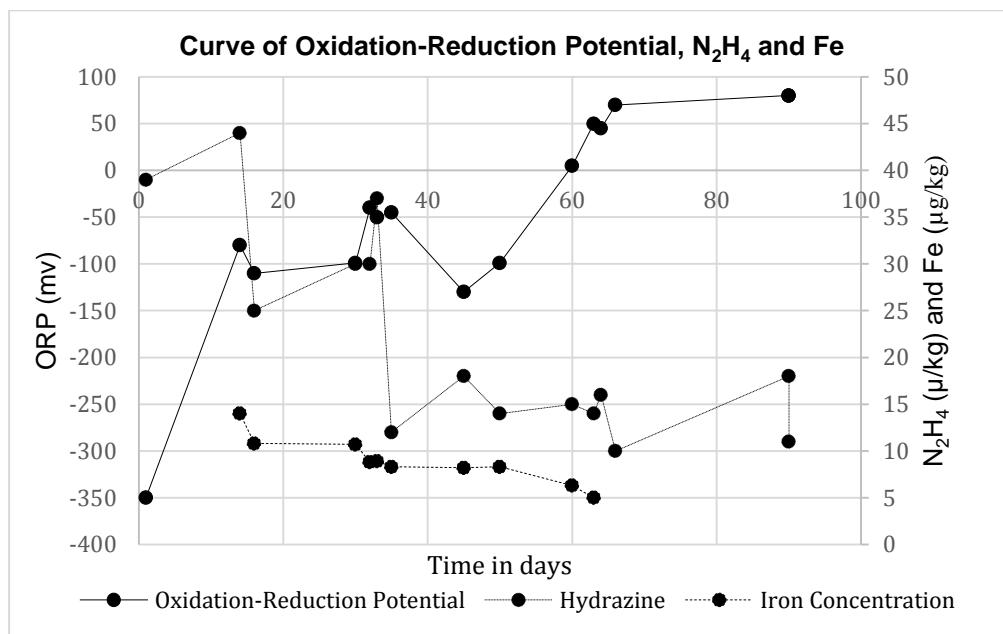
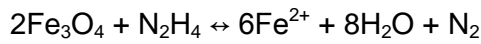


**Figure 1.11: The effect of hydrazine on oxidation-reduction potential and iron concentration**

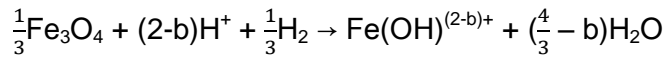
**(Adopted from Guidelines for Controlling Flow-accelerated Corrosion in Fossil and Combined Cycle Plants. EPRI. Palo Alto. CA: 2005. 1008082) [29]**

The graph indicates that hydrazine as a reducing agent can be eliminated to increase the system (ORP) which will decrease FAC and corrosion as indicated by a decrease in iron concentration, this (ORP) would be the main controlling factor in single-phase FAC. Also, the graph indicates that under reducing (hydrazine) conditions, should the (ORP) reduce further it will lead to a further increase in FAC due to magnetite dissolution as follows:





**Equation 1.19**



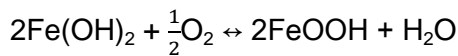
**Equation 1.20**

Reductive-dissolution, this reaction is only important at temperatures above 200 °C where hydrazine undergoes thermal decomposition according to the following equation:

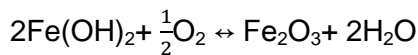


**Equation 1.21**

The decrease in FAC with a decrease in hydrazine is because the elimination of hydrazine raises the free corrosion potential of steel, particularly in the low temperature range of less 150 °C and the ferrous ions leaving the base metal are oxidized to ferric oxide hydrate (FeOOH) or ferric oxide (Fe<sub>2</sub>O<sub>3</sub>) within the pores of the protective layer or at the oxide/water interface:



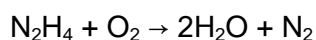
**Equation 1.22**



**Equation 1.23**

The ferric oxide hydrate or ferric oxide then clogs the pores of the porous epitactic protective layer thereby inhibiting diffusion of ferrous ions (Fe<sup>2+</sup>) into the water and reducing corrosion and FAC rates [14].

But because reducing conditions are required for the steam generators, this option cannot be applied. Hydrazine is therefore used for elimination of oxygen and to establish reducing conditions in the feedwater.



**Equation 1.24**

A target feedwater hydrazine concentration of greater than 70  $\mu\text{g N}_2\text{H}_4/\text{kg}$  is maintained for additional protection of the feedwater construction material considering the CEX dissolved oxygen limit of < 10  $\mu\text{g O}_2/\text{kg}$  with the expected value of < 5  $\mu\text{g O}_2/\text{kg}$ . The actual minimum hydrazine limit is 50  $\mu\text{g N}_2\text{H}_4/\text{kg}$ .

1.6.2 Ammonia and ethanolamine application (two-phase FAC)

In a two-phase situation, such as in the drain lines, between the high-pressure turbine and GSS and the exhaust lines of the steam driven feed pumps (APP) as depicted in Figure 2.4, it would not be possible to increase the oxidizing potential (if this option were to be considered) due to practical reasons in which case pH as a secondary controlling factor of the water phase is increased through ammonia, or in some instances a materials solution of replacing components with chromium is applied.

The beneficial impact of increased pH in mitigating FAC is based on the fact that magnetite is soluble in the temperature range of 140 °C – 200 °C with maximum solubility occurring at 150 °C, its solubility decreases as the pH is increased at that temperature as can be seen in Figure 1.12.

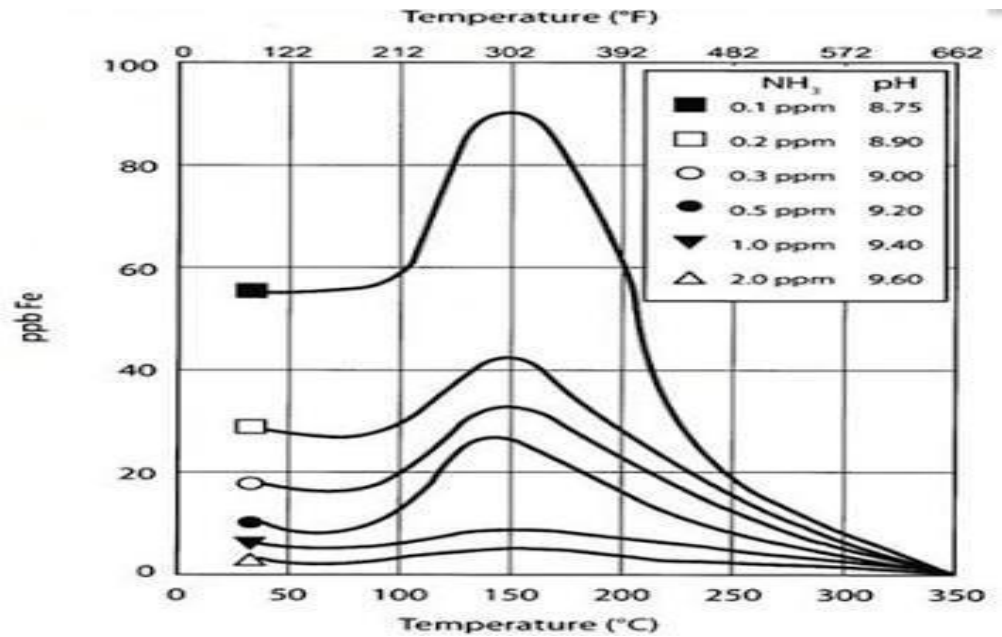


Figure 1.12: Solubility of magnetite as a function of temperature at various ammonia concentrations

**(Adopted from Rhee, H. et al., 2014:432) [30]**

Therefore, the pH being targeted is the pH at temperature ( $pH_{(t)}$ ) maintained at one pH unit above the neutral  $pH_{(n)}$  at that temperature [1]. In the cold temperature region of below 140 °C, the topotactic layer of magnetite is very thin and allows ferrous ions ( $Fe^{2+}$ ) to diffuse easily from the base metal through the pores of the magnetite to the oxide/water phase boundary which then accelerates the corrosion rate of the base steel. The feedwater pH elevation in this temperature region is meant to promote formation of ferrous hydroxide ( $Fe(OH)_2$ ) which transforms very slowly to magnetite in this temperature region [14].

In the beginning of Koeberg operation, there were major FAC issues in the regions in which steam moisture content of > 5 % occurred. To mitigate this, the initial feedwater pH of 9.45 being controlled through ammonia was increased to 9.65. This change in pH led to a significant decrease in FAC estimated to about 50 % but did not eliminate FAC completely due to the volatility of ammonia which favours the steam phase leaving the wet steam regions of the circuit unprotected and still susceptible to FAC.

A move to an alternative amine in a form of ethanolamine (ETA) was proposed, the advantage of ETA over ammonia is its relatively lower volatility which means that it would provide adequate protection in the wet steam regions (two-phase). For example, the pre-ETA treatment feedwater total amount of iron concentration values were typically between  $4\mu g$  Fe/kg and  $6\mu g$  Fe/kg, whereas the current post-ETA values have reduced to between  $1\mu g$  Fe/kg and  $2\mu g$  Fe/kg [35] with the pH being maintained at 9.70 at ETA concentrations of 4mg ETA/kg in the feedwater. Also, a study conducted under simulated secondary water chemistry conditions confirms the reduced corrosion rate for pH under ETA treatment compared to ammonia as can be seen in Figure 2.16 below [15]:

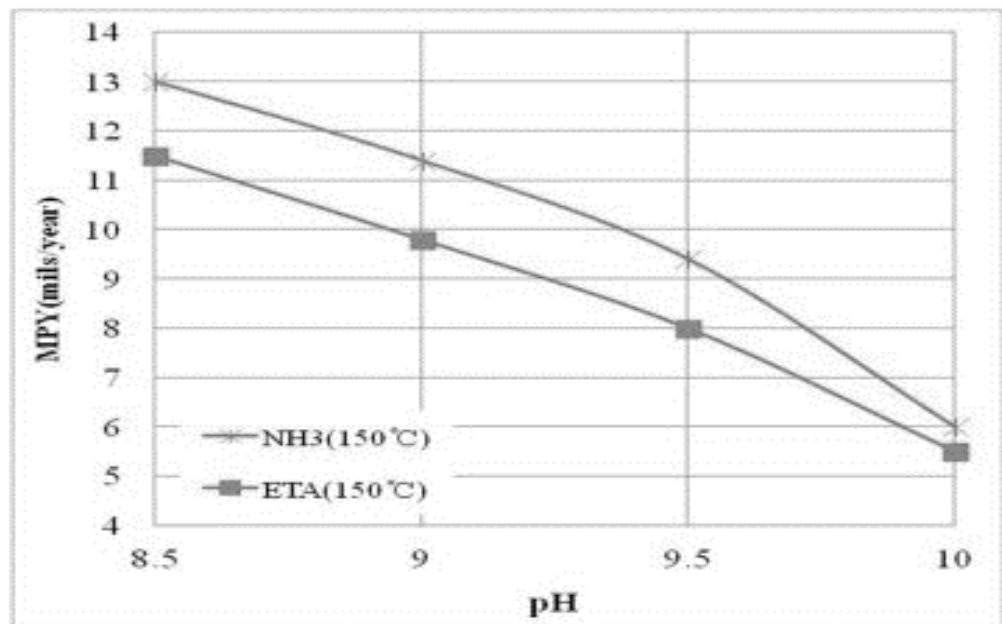


Figure 1.13: Effect of pH on corrosion rate of carbon steel in two chemicals at 150 °C

(Adopted from Rhee, H. et al., 2014:435) [30]

From the same study, a similar decrease in corrosion rate for temperature is observed as affected by ETA in Figure 1.14 below:

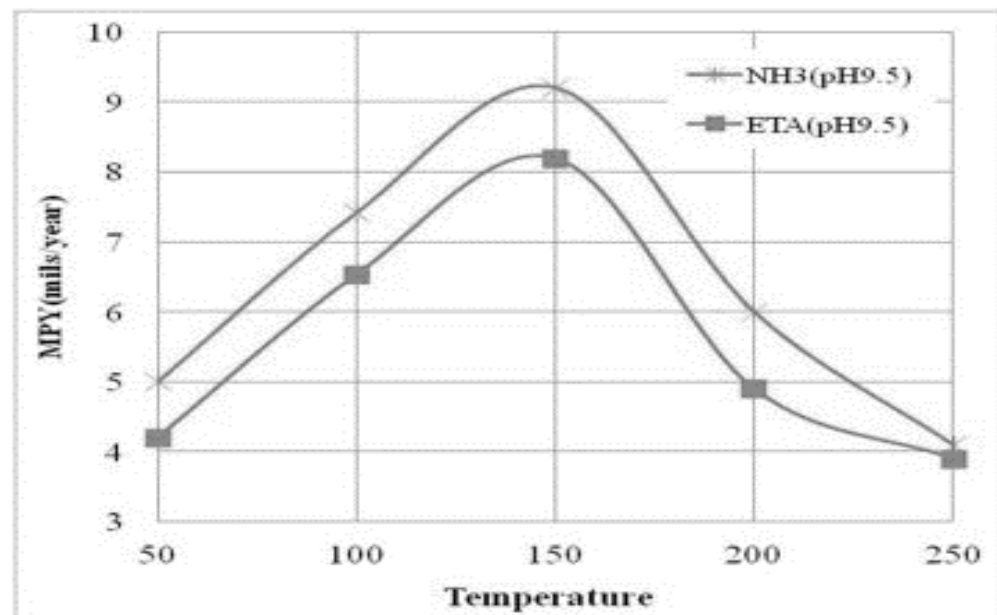


Figure 1.14: Effect of temperature on corrosion rate of carbon steel in two different chemicals at pH 9.5

(Adopted from Rhee, H. et al., 2014:435) [30]

The study concludes that the reasons for this ETA impact upon corrosion rates are lower diffusion coefficients and electrical conductivities, highly concentrated hydroxide ions with higher pH that consumes more protons and catalysis of oxide layer formation on metal surfaces that subsequently blocks transport of electrons and intrusion of impurities.

### 1.6.3 Effect of impurities on FAC

Sources of impurities into the feedwater system includes municipal water supply which contains organic halides, inorganic minerals such as calcium, magnesium, and sodium. The anions include sulphates, chlorides, silicates, carbonates, and bicarbonates together with organic matter. Most of these impurities are removed by charcoal filtration, followed by ion-exchange in the demineralised water production plant to produce ultra-pure water in accordance with the specification document. Unfortunately, chlorides and sulphates make their way through the demineralization process because some of them exist in the supply water as part of organic compounds, these compounds are trihalomethanes for which the demineralization process was not designed for. However, these compounds only decompose at high temperatures in the steam generators releasing the bound chlorides and sulphates into the steam generator water. Concentrations of 20  $\mu\text{g Cl}^-/\text{kg}$  and 5  $\mu\text{g SO}_4^{2-}/\text{kg}$  have been observed in situations of high condenser make-up water volumes whereas typically values are around 0.80  $\mu\text{g Cl}^-/\text{kg}$  and 0.30  $\mu\text{g SO}_4^{2-}/\text{kg}$ .

Other sources can be the chemicals that are used in the maintenance work performed on certain plant equipment, particularly major overhauls of the main feedwater pumps.

Sea water is another possible source in case of condenser tube leaks, common impurities are sulphates ( $\text{SO}_4^{2-}$ ), chlorides ( $\text{Cl}^-$ ), carbonates ( $\text{CO}_3^{2-}$ ), bicarbonates ( $\text{H}^+\text{CO}_3^-$ ), sodium ( $\text{Na}^+$ ), magnesium ( $\text{Mg}^{+2}$ ) and calcium ( $\text{Ca}^{+2}$ ).

It has been determined that the anion impurities have an influence on FAC, corrosion mechanisms and rates together with oxide morphology. For example, the one EDF model gives FAC rate in terms of the following simplified expression:

$$\text{FAC rate} = 2 \cdot K \cdot \Theta \cdot C_{\text{eq}}$$

#### Equation 1.25

- K is the mass transfer coefficient
- $\Theta$  the oxide porosity
- $C_{\text{eq}}$  the soluble ferrous ion concentration at equilibrium with the magnetite

The model considers in its description of FAC, the soluble ferrous ion production from metal oxidation at the iron-magnetite interface and dissolution-reduction of magnetite at the oxide-water interface followed by mass transfer of the ferrous ions into the bulk water.

Since magnetite on the surface of the metal is composed of a dense topotactic layer and a porous epitactic layer on top, ferrous ions from the metal surface diffuses through the pores of the oxide towards the bulk water resulting in a positive charge build-up within the pores. Also, the anion impurities from the bulk water diffuse into these pores and maintain electroneutrality thereby encouraging further corrosion of the base metal, resulting in an increase in bulk water ferrous ion concentration. If the concentrations of chlorides ( $\text{Cl}^-$ ) and sulphates ( $\text{SO}_4^{2-}$ ) are high, the pH within the oxide will be lower therefore ferrous ions will remain in solution. In contrast, if the concentrations of carbonates ( $\text{CO}_3^{2-}$ ) and bicarbonates ( $\text{H}^+\text{CO}_3^-$ ) dominates, the pH within the pores will be higher and there will be a possibility of  $\text{FeCO}_3$  formation which might impede ferrous ion diffusion towards the bulk water [32].

In addition to their impact on FAC and corrosion rates, the anion impurities can affect the morphology of oxides. Iron oxides exhibit a variety of crystal morphologies and crystalline sizes and a variety of possible transformation between different phases, and the most commonly occurring phases of iron oxides in power plants are as given in Table 1.2 below [23]:

**Table 1.2: Eight forms of iron oxides and oxyhydroxides**

| Oxyhydroxides         |                | Oxides   |              |
|-----------------------|----------------|--|--------------|
| Formula               | Name           | Formula  | Name         |
| $\alpha\text{-FeOOH}$ | Goethite       | $\text{Fe}_5\text{OH}_8 \cdot 4\text{H}_2\text{O}$ | Ferrihydrite |
| $\beta\text{-FeOOH}$  | Akaganite      | $\alpha\text{-Fe}_2\text{O}_3$                     | Hematite     |
| $\gamma\text{-FeOOH}$ | Lepidocrocite  | $\gamma\text{-Fe}_2\text{O}_3$                     | Maghemite    |
| $\delta\text{-FeOOH}$ | Ferrosyhydrate | $\text{Fe}_3\text{O}_4$                            | Magnetite    |

**(Adapted from Namduri H, 2007:19) [23]**

In their study, Sarin et al. (2002:365) states that because oxidation of ferrous ions ( $\text{Fe}^{+2}$ ) is one of the primary routes for corrosion scale formation, anions that forms complexes with dissolved iron can have an effect on the composition/morphology of the scale [32]. In this study, together with another separate study by Taylor, R.M. (1984:175), it is reported that the chloride promoted formation of lepidocrocite ( $\gamma\text{-FeOOH}$ ). Furthermore, the effect of chloride ( $\text{Cl}^-$ ) could retard the formation of magnetite due to surface hydroxide ( $\text{OH}^-$ ) being partially replaced by chloride either during the initial formation of the intermediate green  $\text{Fe}^{+2}/\text{Fe}^{+3}$  hydroxy chloride phase or during its subsequent oxidation where it transforms to lepidocrocite or magnetite.

This replacement of hydroxide by chloride hinders water elimination by condensation of the neighbouring hydroxide and the formation of Fe-O-Fe bonds necessary for the magnetite [34]. The sulphates are said to have a goethite forming effect during the oxidation of Fe(OH)<sub>2</sub>. It is evident from this that oxide morphology can be altered by a presence of anion impurities which will impact on FAC and corrosion rates.

## **CHAPTER 2**

### **RESEARCH OVERVIEW**

#### **2.1 Research problem statement**

The startup transport amount of corrosion products at Koeberg nuclear power station has never been previously quantified since the beginning of plant operation. This means that it is not known how much of the startup amount accounts for the total fuel cycle amount. The total mass of sludge retrieved from outage to outage vary depending on various plant operational & chemistry factors. However, it has never been demonstrated how much of this total mass originates from the startup. Knowing the startup amount is important because it will inform the station of whether it is necessary to institute clean-up interventions to minimize start-up transport amounts depending on the findings.

#### **2.2 Research questions**

The following questions are posed to aid the research study and with respect to corrosion product transport during a plant start-up. What are the concentration values of corrosion products in the form of iron during the phase of plant startup? What happens to the concentration values of corrosion products as reactor power increases, and how do they compare when the reactor power is less than 30 % and above up until 100 %? Can the transported amount provide some indication as to the effectiveness of chemistry control during the startup phase? Also, can the transported amount serve to highlight the general efficiency of lay-up practices during outages?

#### **2.3 Research aims and objectives**

The aim of this study is to take samples of corrosion products on the secondary feedwater plant during plant startup. These samples will be taken at pre-determined frequencies using integrator samplers that are installed on strategic locations on the plant. Also, part of the aim is to digest these samples using heat and acid digestion.

The reason for digesting the samples is to dissolve the filters and most importantly, to dissolve solid particles to get them into solution for the purpose of analysis by the chosen method of atomic absorption spectrophotometer. Lastly, the aim is to then analyses these samples to determine the concentration of iron, whose values will be used in the transport calculations. From these aims and the stated research problem, the objective of this study will be to evaluate and quantify the amount of transported corrosion products during plant start-up and their contribution to the total fuel cycle amount. This will make it possible to answer these questions and resolve the research problem.



## **2.4 Research hypothesis**

During normal and steady state operation of the plant, the typical concentration values for corrosion products in the secondary feedwater system is about 1.0 µg/kg, with almost no iron oxide colouration on the sample filters. However, during a plant transient, which closely replicates a startup situation, heavy colouration of sample filters is observed with an accompanied increase in iron concentrations values to about 10 µg/kg.

Now, given the similarities between plant transients and startups with the added outage factor and the quoted values from literature, it is expected that the concentration values of iron will be high to above 10 µg/kg. It is therefore expected that transport amounts of corrosion products for the startup phase will equally be high and will contribute significantly to the total amount for the fuel cycle.

## **2.5 Research scope and delimitation**

This research study will only be conducted and therefore be limited to the secondary heat transfer loop of Koeberg's operating Unit 2 and for the startup of cycle 18. Therefore, the results obtained from the study will only be applicable to this unit and for the specified cycle since each unit and cycle is unique in terms of its chemistry behaviours, operational practices, mass of sludge retrieved from the steam generators and many other factors.

The sampling will only commence after the feedwater flow is changed over directly to the steam generators coming from the main condenser and through the feedheaters. What this means is that, nothing will be known about the amount of corrosion products emanating from the condenser prior to the change-over. This point should not be trivial because it would in any case lead to over estimation as these amounts do not find way to the steam generators anyway. Also, most of the solids are removed from the condenser water by the condensate polishing plant which uses ion-exchange resins to clean the water. This is done so that the water can meet the chemistry specifications to be fit for use in the steam generators.

The study will not attempt to identify the exact point of origin and contribution to the transported amounts of corrosion products from different parts of the secondary feedwater plant. However, the position of the selected sample point is such that it will collect all the transported corrosion products along the secondary feedwater system from the start point. This point was chosen because it is located downstream of the last feedheaters before the water makes its way to the steam generators.

Because the startup is a highly dynamic and forward/once off event, it will not be possible to replicate data to check reproducibility. This limitation will make it impossible to make certain statistical statements about the data and the study itself.

## **2.6 Research method**

### 2.6.1 Literature review

Literature survey was conducted to establish what is being done across the nuclear industry with respect to corrosion product transport evaluation during start-up and its contribution to cycle transport.

### 2.6.2 Data collection

Data will be collected by placing a set of 0,45 µm nitro-cellulose and a 0,45 µm resin impregnated filters into the corrosion product samplers to collect both particulate and soluble iron respectively. Given that data will be collected at different shifts by different personnel, the following instructions will be given to both the plant chemistry and analytical chemistry personnel.

#### Plant Chemistry

- As soon as the condenser goes on long recirculation, establish sample flow on AHP2 and 2CEX sampling lines to the corrosion product monitors for flushing until the first sets of filters are placed
- Place filters on 2CEX and AHP2 immediately after feed supply to steam generators is changed over from ASG to ARE, the shift chemist or coordinator to advise the analyst on shift.

Remove the filters after 2 hours, place new filters and sample for 4 hours, the next one for 8 hours, 16 hours, 24 hours after which the last filters should be left until the unit reaches 30 % reactor power from which the normal 7 day sampling period must be followed for the entire fuel cycle (1 year 3 months). The reason for shorter sampling periods during the startup phase is that high levels of corrosion products were expected, while for the fuel cycle at steady state operation lower amounts were expected, hence longer sampling periods.

#### Analytical Chemistry

Analytical chemistry to digest and analyse all the samples for iron concentration as per procedure and fill in Table 2.1.

**Table 2.1: Template for sample results**

| Sampling Period | Results   |   |
|-----------------|---|---|
|                 | AHP2 (Fe)   | 2CEX (Fe)   |
|                 | AA results / integrator volumes in litres ( $v_1/v_2$ ) | AA results / integrator volumes in litres ( $v_1/v_2$ ) |
|                 | mg/kg   | mg/kg   |
|                 | T =   | T =   |
|                 | B =   | B =   |
|                 | $V_1 =$   | $V_1 =$   |
|                 | $V_2 =$   | $V_2 =$   |

### 2.6.3 Sample treatment

There are several methods for digesting resin impregnated and cellulose filters, which includes microwave digestion, laser, ashing and other methods. Acid digestion method was chosen as it was the only one available at Koeberg. Sample filters will be taken to the laboratory and photographed, acid digested separately and analysed for soluble and particulate iron concentrations.

### Sample analysis

There are various analytical techniques for the analysis and quantification of iron in aqueous systems, examples include ICP-OES, X-Ray spectrometry & voltammetry/polarography. However, at Koeberg atomic absorption spectrophotometer (flame & furnace) is routinely used to analyse and quantify iron in various plant systems and at concentrations levels expected in this study. This was the instrument of choice due to availability, expected concentration levels in the startup samples, ease of use and that it meets the required levels of accuracy for the purpose of this study.

### 2.6.4 Transport calculations

Iron concentration results in mg/kg as obtained directly from the instrument will be converted to  $\mu\text{g/kg}$ , which will then be used to evaluate transport amounts below 30 % reactor power, cumulative amounts above 30 % up to 100 % reactor power and for the entire fuel cycle. The start-up phase was defined in terms of two windows to form a startup transport basis, time zero window which covers reactor power of < 30 % and 11 days startup window, which is the average time it takes to reach 100 % reactor power.

The following approach will be used to estimate the contribution of iron transport amounts due to startup:

- Cycle transport following the startup was calculated.
- Based on the calculated cycle transport, a curve of cumulative transport versus time at steady state following the startup was constructed.
- From the curve of cumulative transport versus time, an extrapolation to time zero was made to determine the startup transport amount for the < 30 % reactor power window as defined.
- The transport amount for the 11 days startup window was calculated, this was then added to the amount obtained for the < 30 % reactor power window to arrive at the total startup transport amount.
- The extrapolated value from the cumulative curve to time zero was compared with the calculated transport amount based on the corrosion product sample concentrations obtained below 30 % reactor power.

#### 2.6.5 Data treatment (statistics)

From the plotted curve of cumulative transport versus time, a method of least squares will be used to find the best fit line or regression line through the data from which the amount (kg) at time zero ( $x_i = 0$ ) will be estimated. This will be followed by working out of the regression coefficient to test that the regression model fits the data. Finally, the standard error of the estimate (startup transport amount) will be expressed.

## CHAPTER 3

### LITERATURE REVIEW

Various nuclear power plants have sampled and evaluated corrosion products during plant startup, with the intention to understand their contribution to the total transported amounts during a fuel cycle, different amounts are reported from plant to plant. High levels of  $\gamma$ -FeOOH were observed in one start-up suggesting that active corrosion is still occurring during this phase. Another estimate suggests that 50 % or more of the total corrosion product transport could arise from transients but field data is variable. It is reported that generally the major contribution during start-up is from the forward drains pumps (ACO) and feedheaters (RP1 to AHP2) [33].

Therefore, the indication from literature is that there is no consistent data across industry; the results differ from one plant to the other and from one startup to the next. There are various contributing factors to this which includes operational factors, plant construction materials, wet conservation practices during shutdown periods, startup chemistry conditions etc.

Hook et.al. in their study conducted at Florida Power & Light's Port Everglades station observes that corrosion product concentrations tend to spike during plant start-ups. Concentrations of up to 10 – 100 times higher than those for normal operations are reported, with values ten times higher during start-ups following shutdowns in which condenser vacuum was not maintained. The authors attribute most of the effects to chemistry parameters such as oxygen, pH and hydrazine and operational changes. The reported iron transport rates during start-up are 200 g/hr for condensate (CEX) and 190 g/hr for No.6 feed heater (AHP2 equivalent) outlet respectively. They also report that iron was transported predominantly in particulate form [18].

In a study by EPRI for one plant, estimates of about 24 kg of iron transported during startup were reported, while 0.23 kg for another plant were reported. However, it is mentioned that for cases where startup transport is very low such as for Plant B, accuracy of estimates was decreased [8]. Fruzetti K in a review carried out for EPRI in 2009 to review start-up iron transport from 21 plants concluded that the amount of iron transported during the start-up varied from 1.82 kg – 36.32 kg with a median value of about 6.81 kg, the total estimated iron transport during the fuel cycle ranged from approximately 45.4 kg – 227 kg. A sample of results for these findings is listed in Table 3.1 below [29].

**Table 3.1: EPRI Survey Results**

| Plant | Database   | Startup Transport basis, days | Startup Transport, kg | Cycle Transport, kg | Startup Transport, % |
|-------|------------|-------------------------------|-----------------------|---------------------|----------------------|
| D     | Full Cycle | 10                            | 2.68 kg               | 58.97 kg            | 5                    |
| E     | Full Cycle | 13                            | 5.72 kg               | 102.06 kg           | 6                    |
| F     | Full Cycle | 10                            | 38.1 kg               | 190.06 kg           | 20                   |
| I     | Full Cycle | 10                            | 28.12 kg              | 229.06 kg           | 12                   |

**(Adapted from Pressurized Water Reactor Secondary Water Chemistry Guidelines (Rev 7). EPRI, Palo Alto, CA: 2009. 1016555) [29]**

Koeberg has established a program in which tube sheet lancing (TSL) is performed at the end of every operating fuel cycle to remove sludge on top of tube sheet and this amount is weighed to determine its mass for each fuel cycle [10], see Figure 3.1:

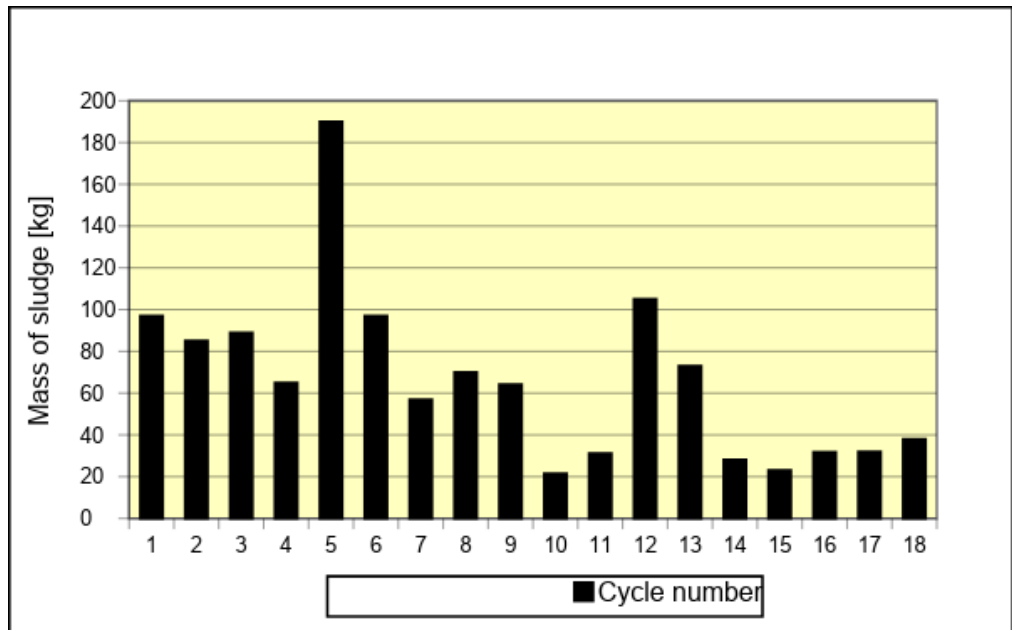


**Figure 3.1: Total mass of steam generator sludge per fuel cycle**

Figure 3.1 shows a general decrease in sludge mass with increases for specific fuel cycles which are accounted for by plant incidents, such as cycle number 12 where a net was burnt over the main condenser during the outage. Organic pollution was introduced into the steam generators through feedwater from the main condenser, making it difficult to maintain certain important chemistry parameters within operational limits. The condensate polishing plant was then placed in-service for extended periods; the result was an increased amount of corrosion products hence an increase in sludge mass.

In addition to the mass, sludge samples are taken for elemental analysis and Mossbauer spectra determination. Both elemental and Mossbauer results are given in Table 3.2 and Table 3.3 respectively, followed by a brief discussion for each.

**Table 3.2: Elemental analysis of sludge sample**

| Determination  | Result | Units   | Method used                   |
|----------------|--------|---------|-------------------------------|
| Carbon         | 0.11   | % (m/m) | carbon and sulphur combustion |
| Aluminium (Al) | 945    | mg/kg   | ICP-OES                       |
| Arsenic (As)   | < 70   | mg/kg   | ICP-OES                       |
| Boron (B)      | < 53   | mg/kg   | ICP-OES                       |
| Calcium (Ca)   | 470    | mg/kg   | ICP-OES                       |
| Chromium (Cr)  | 374    | mg/kg   | ICP-OES                       |
| Cobalt (Co)    | 121    | mg/kg   | ICP-OES                       |
| Copper (Cu)    | 1.02   | % (m/m) | ICP-OES                       |
| Iron (Fe)      | 71.1   | % (m/m) | ICP-OES                       |
| Lead (Pb)      | < 70   | mg/kg   | ICP-OES                       |
| Lithium (Li)   | 5.7    | mg/kg   | ICP-OES                       |
| Magnesium (Mg) | 2.5    | mg/kg   | ICP-OES                       |
| Manganese (Mn) | 1.31   | % (m/m) | ICP-OES                       |
| Nickel (Ni)    | 0.32   | % (m/m) | ICP-OES                       |
| Phosphorus (P) | 0.12   | % (m/m) | ICP-OES                       |
| Potassium (K)  | < 70   | mg/kg   | ICP-OES                       |
| Silver (Ag)    | < 70   | mg/kg   | ICP-OES                       |
| Silicon (Si)   | 929    | mg/kg   | ICP-OES                       |
| Sodium (Na)    | < 70   | mg/kg   | ICP-OES                       |
| Tin (Sn)       | 221    | mg/kg   | ICP-OES                       |
| Titanium (Ti)  | 142    | mg/kg   | ICP-OES                       |
| Zinc (Zn)      | 0.50   | % (m/m) | ICP-OES                       |
| Zirconium (Zr) | < 70   | mg/kg   | ICP-OES                       |

**(Adapted from Hudson-Lamb, D.C & Van Niekerk, W.G, 2011:2) [19]**

Plant equipment such as GSS experiences material loss due to steam erosion around the nose cone of the tube bundle. The damaged areas are typically rehabilitated using the arc spray process which consists of surface preparation, surface coating and application of a sealant. Two surface preparation materials are used, blastrite platinum grit which contains silica (90% SiO<sub>2</sub>). Aluminium oxide grit (92 % Al<sub>2</sub>O<sub>3</sub>, 2.8 % TiO<sub>2</sub>, 1.9 % SiO<sub>2</sub>, 2.2 % Fe<sub>2</sub>O<sub>3</sub>) is also used for improving grit hardness due to its titanium content, this is for surface finishing. A bond layer consisting of Metco 8405 (80 % Ni, 20 % Al) is applied for the coating step. The final step consists of applying Metcoseal as a sealant, which is a phenol based organic compound [2].

Given that the GSS drains cascades to ACO from which they are pumped into the feedwater towards the steam generators, it is evident that significant amounts of titanium (Ti), silicon (Si) and Aluminium (Al) originates from GSS following outage in which arc spraying was performed. Cobalt (Co), chromium (Cr) and lithium (Li) can be related to primary water leak into the steam generator secondary water due to a known number of small cracks in the tubes, chromium is also found in some stainless-steel replacement components in the secondary feedwater. Copper (Cu) is a constituent of some of the GSS tubing material, turbine gland steam condenser, the condensers of vacuum pumps and impellers of the extraction pumps. Calcium and Magnesium could be from the make-up water or due to historical sea water leaks into the feedwater through condenser tubes leaks. Iron (Fe) is as expected due to the construction material of the secondary circuit being “all-ferrous” and iron find its way through to the steam generators from corrosion product transport.

The Mossbauer spectral analysis also confirms that the sludge is mostly composed of magnetite given the distribution of Fe<sup>+2</sup> and Fe<sup>+3</sup> in the oxide “holes”/sites, this was also supported by visual observation of the black colour of the sludge

**Table 3.3: Mossbauer spectral components for sludge at room temperature**

| Sample                 | Spectral component   | T, Line width | <sup>δ</sup> /Fe (mm/s) | QS (mm/s) | B <sub>hf</sub> (T) | Abundance |
|------------------------|--|---------------|-------------------------|-----------|---------------------|-----------|
| Outage 218<br>May 2011 | Sextet1<br>(tetrahedral A-site) Fe <sup>+3</sup>                     | 0.32          | 0.29                    | 0.0       | 49.2                | 37 (1)    |
|                        | Sextet2<br>(Octahedral B-site)<br>Fe <sup>+2</sup> /Fe <sup>+3</sup> | 0.48          | 0.66                    | 0.0       | 45.8                | 63 (1)    |

(Adapted from Hearne, G.R, 2011:4) [17]

Most feedwater corrosion products (usually dissolved iron) deposit in the steam generators labelled SG in Figure 2.2 and build magnetite scales on the heat transfer tube surfaces causing fouling, which a degradation in primary to secondary heat transfer. Corrosion products also accumulate within heat transfer crevices such as tube to tube support (TSP) and at tube to tube sheet (TTS) creating blocked crevices.

It is estimated that 5 – 10 % of feedwater corrosion products accumulate at tube to tube sheet building hard caked deposits. These blocked heat transfer crevices and TTS hard deposits are the special locations where the feedwater salt impurities preferentially concentrate and may cause tube corrosion.



The magnetite deposited at the TTS is called sludge; the deposits will grow over time during plant operation and build thick caked sludge. Figure 3.2 shows the TTS and TSP locations within a PWR steam generator while Figure 3.3 shows the extent of sludge build up.

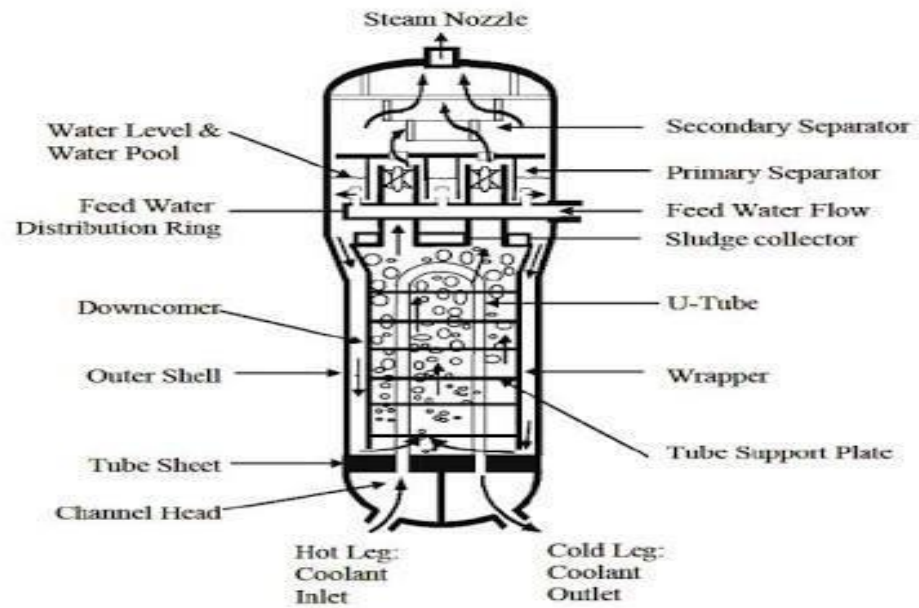


**Figure 3.2: Schematic of vertical PWR steam generator**

(Adopted from Bonavigo, L. & De Salve, M, 2011:374) [6]

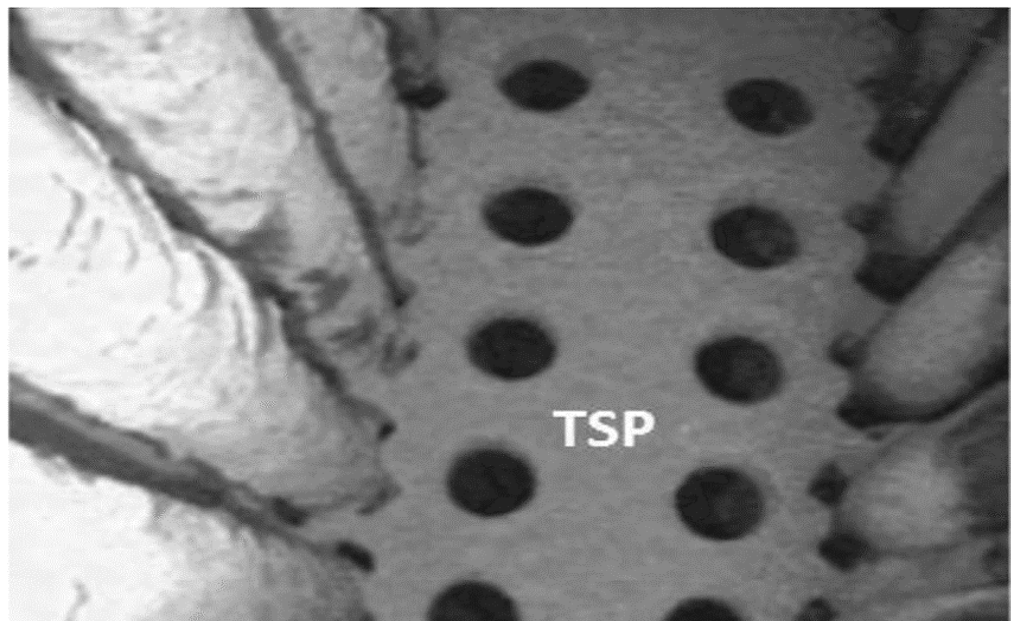


**Figure 3.3: Sludge build up on tube support plate and on the tubes**

(Adopted from [www.sciencedirect.com/science/article/pii/S002954931300280X](http://www.sciencedirect.com/science/article/pii/S002954931300280X)) [37]

Nordmann and Odar (2010:8) mentions that according to the work performed by Atomic Energy of Canada Limited (AECL) in collaboration with EPRI, the rate of tube fouling is strongly dependent upon surface chemistry of the corrosion products and amine used for pH control. They further note that hematite and lepidocrocite's fouling rates far exceeds those of magnetite ( $\text{Fe}_3\text{O}_4$ ) under identical operating conditions, this is attributed to surface charge sign given that the steam generator tube material (Alloy 600MA) heat surface has a negative charge at operating temperature while magnetite has negative charge with a positive charge for both hematite ( $\text{Fe}_2\text{O}_3$ ) and lepidocrocite ( $\gamma\text{-FeOOH}$ ). Some plants were reported to have observed increased tube fouling just after plant startup operation and this was correlated to increased oxygen concentrations during start-up [24]. This is supported in another study in which high levels of lepidocrocite ( $\gamma\text{-FeOOH}$ ) were observed during start-up [33].

Regarding hide-out phenomenon, there are various mechanisms by which salt impurities in the bulk feedwater can concentrate within the steam generators and they are:

- adsorption of impurities onto metal oxide surfaces and in particular the polyvalent anions such as sulphate ( $\text{SO}_4^{-2}$ ) and phosphate ( $\text{PO}_4^{-3}$ ). This mechanism occurs during heat-up and power production whereby impurity uptake onto the oxide surface is a function of surface area and bulk water concentration,
- concentration of impurities in flow restricted geometries such as TTS and TSP crevices whereby the local environment has a concentrated liquid, steam and precipitates resulting when solution concentrates beyond solubility limits of certain species and can cause localized corrosion, and
- concentration of impurities within the cylindrical pores of the deposited oxides through convective or diffusion transport process [27].

A reverse process of hide-out return also occurs when heat flux is sufficiently reduced to the point where boiling concentrates impurities at a rate lower than that with which they can be removed by diffusion and/or liquid entrainment. This reverse process is observed during plant transients and shutdown from normal power operation.

In the accelerator industry, corrosion products can affect accelerator reliability and operation similar to how it did at the diamond light source Ltd company (DLS).The accelerator's synchrotron facility and its magnets contain copper and stainless-steel and cooling is achieved by use of low dissolved oxygen, low conductivity and alkaline demineralised water to minimise oxide formation. The dissolved oxygen excursions are said to maximize the corrosion rate and hence particle release believed to be related to a change in the balance

between copper I and copper II oxides, possibly by phase changes between the two oxides affecting their ability to adhere to surfaces.

The accelerator experienced various issues including discolouration of the transparent plastic bodies of rotameter flow meters, control valves clogged with copper oxide causing low flows, clogging of cooling water components thereby reducing water flow to the point where low flow alarms were causing machine downtime. Chemical analysis of the deposits using the Xanes (X-ray absorption near edge structure) Beam line proved that the deposit consists entirely of CuO corrosion products [16].

In the transport industry, concrete structures are reinforced by use of steel and when it corrodes it forms corrosion products that expands and increase the occupied volume within the concrete structure, thereby generating tensile stresses leading to cracks and structural degradation which is very costly. Water to cement ratio affects the extent of penetration of corrosion products into the mortar and hence their concentrations at a given location from the reinforcement bar. Another factor is the impact of corrosion rate on the location-dependent concentration of corrosion products. In one application, X-ray attenuation is used to quantify the total concentration of corrosion products within the mortar as a function of location [25].

In the archaeological and artistic works, silver has found usage in the manufacturing of precious objects such as silver staining of glasses, photographic technology, and electric/electronic technologies. The formation of corrosion products on these artefacts due to corrosion necessitates their conservation and restoration for cultural interest which depends on the knowledge of both their physical and degradation processes, this knowledge can be established by use of Micro-Raman spectroscopy as an analytical technique as it can detect chemical species forming on silver surfaces. It can also distinguish between crystalline forms of corrosion products and chemisorbed species which are said to be related to the secondary processes of corrosion [22].

## CHAPTER 4

### EXPERIMENTAL

#### 4.1 Apparatus

Spanner (11/16 inch), Allen key, tweezers, 0,45  $\mu\text{m}$  nitro-cellulose filter (Whatman 47 mm), 0,45  $\mu\text{m}$  resin impregnated filter (47 mm), Whatman No. 4 filter paper (11,0 cm), petri dish, plastic bottle, 400 ml glass beakers, 100 ml stoppered volumetric flasks, hot plate, drying oven, analytical balance, funnel, digital camera, mini tripod, watch glass.

#### 4.2 Reagents

Conc.  $\text{H}_2\text{SO}_4$ , Conc.  $\text{HNO}_3$  (spectrosol), demineralised water and iron sulphate stock solution

#### 4.3 Instrumentation

Perkin Elmer 7000 Atomic Absorption Spectrophotometer

#### 4.4 Placing of filters (refer to Figure 4.1)

As soon as the condenser water clean-up process was initiated, flows on the sample lines leading to the corrosion product monitors were established on both systems (AHP2 and 2CEX) in order to flush and condition the sample lines and stabilize particulates along the sample lines. The flushing was done for a period of eleven days prior to placing of the first set of filter papers, the benefit of flushing for eleven days was derived from outage delays. Sample filters were placed immediately after feedwater supply to the steam generators was established directly from the condenser when the condenser water quality specifications ( $\text{O}_2$ , cation conductivity and  $\text{Na}^+$ ) were met.

The filter holder inlet tubing assembly was removed from the sample station panel bulkhead fitting and from the filter holder inlet elbow, and by using tweezers, a 0,45  $\mu\text{m}$  nitro-cellulose and two 0,45  $\mu\text{m}$  resin-impregnated filters were placed in the filter holder with the shiny side facing downwards and the smooth side facing down respectively.

The filter holder was then re-assembled, and the inlet tubing replaced followed by tightening both the filter holder bolts and inlet connections. Once the date, time and the volume reading on the totaliser were recorded, the pressure regulator was slightly opened (turning in a clockwise direction) and V3 completely opened with pressure maintained in the range 25 – 30 psi and flow adjusted to 100 – 150 ml/minute using V4. The flowrate and time were recorded.

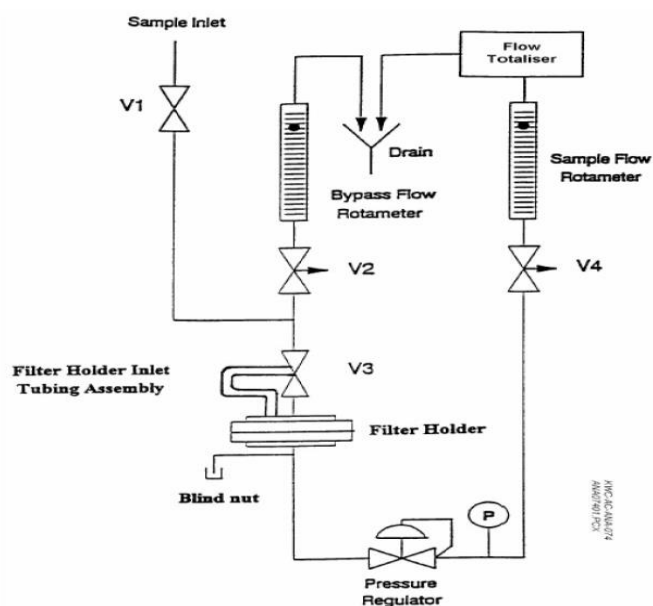


**Figure 4.1: Corrosion product sampler flow diagram**

#### 4.5 Retrieval of Filters

The flowrate was recorded, pressured reduced and V3 closed to stop sample flow followed by recording of the volume, date, and time of the sample. The filter holder inlet tubing assembly was removed from the sample station panel bulkhead fitting and from the filter holder inlet elbow followed by removal of the blind nut from the tee at the bottom of the filter holder.

By use of tweezers, filters were carefully removed and placed into a labelled petri dish. The filter holder was re-assembled, and the filter holder inlet tubing assembly replaced. Secure the filter holder was secured by completely tightening opposite pairs of all bolts and the inlet connections. the date, time and the volume reading on the totaliser were recorded and the top filter photographed within one hour of retrieval.

#### 4.6 Digestion of filters

The nitro-cellulose filter for the insoluble and the two resin impregnated filters for soluble were separated by using tweezers into two labelled 400 ml glass beakers and their respective blanks into their own beakers. 15 ml spectrosol  $\text{HNO}_3$  (conc.) and 10 ml  $\text{H}_2\text{SO}_4$  (conc.) were carefully added to each beaker, all beakers were covered by a watchglass and heated on a hot plate with a gentle boil for 15 minutes after which they were removed and allowed to cool completely. The insoluble contents were transferred with thorough rinsing into a 100 ml volumetric flask containing 20 ml of Milli-Q water and labelled "insoluble".

Using a Whatman No. 4 filter paper, the contents of the glass beaker labelled “soluble” were transferred through filtration into a labelled “soluble” 100 ml volumetric flask containing 20 ml of Milli-Q water. All the solutions were allowed to cool to room temperature, made up to the 100ml mark with Milli-Q water and analysed for Fe.

#### 4.7 Sample analysis

Atomic absorption flame was used a method of analysis. Atomic spectroscopy takes advantage of the processes that occurs when light interacts with matter in which light as electromagnetic radiation is absorbed by atoms of a specific element. The amount of light absorbed will be a function of the number of individual ground state atoms produced in the process, their concentration is then determined by comparing the absorbance of the sample to that of known standard concentrations (calibration).The linear relationship between concentration and absorbance is expressed by the Beer-Lambert law as follows:

$$A = \epsilon \cdot b \cdot c$$

- $\epsilon$  is the molar absorptivity (unique for each element)
- $b$  length of light path intercepted by the sample cell in cm
- $c$  concentration of sample



Perkin Elmer 700 Atomic Absorption Spectrophotometer

**Figure 4.2: Perkin Elmer 700 Atomic Absorption Spectrophotometer**

**(Adopted from Makapela, G.A, 2012:7) [21]**

Standard solutions with the same matrix as the sample were prepared in the same range as the sample and where applicable samples were diluted to the range of the standards. After each sample was run, a 5 % nitric acid solution was aspirated to prevent contamination of the previous sample.

**NOTE:** Refer to the Appendix A for recommended conditions

#### 4.7.1 **Flame setup**

The **WinLab32for AA** program was initiated from the PC by clicking on it, a step which prompted the system to initialise the installed components. The stored method was selected from the file followed by clicking on the lamp icon, which was switched on to energise and allowed to warm up for 15 minutes after which the lamp was optimised.

The burner head position was optimised by igniting the flame and allowing it to burn for 5 minutes to allow the burner head to reach optimum conditions. A blank was aspirated to autozero the instrument followed by aspiration of a standard solution for sensitivity check that was adjusted to the absorbance of 0.20 absorbance units by adjusting both the nebuliser and burner head.

#### 4.7.2 **Analysis**

The flame was ignited, and the de-ionized water aspirated followed by autozeroing the graph. The blank was analysed and zeroed before running the standards. A set of standards were run followed by the samples and quality control solutions. After all the samples were run and results obtained, the lamp was switched off and the flame extinguished.

## CHAPTER 5 RESULTS

### 5.1 Raw data for reactor power < 30 %

**Table 5.1: AHP2 and 2CEX iron concentration results**

| Sampling period                                       | System / Results  |             |        |   |             |         |
|---|---|-------------|--------|---|-------------|---------|
|   | AHP2 (Fe)   |             |        | 2CEX (Fe)   |             |         |
|   | AA results / integrator volumes in litres (V <sub>1</sub> /V <sub>2</sub> ) | Calculated  | Total  | AA results / integrator volumes in litres (V <sub>1</sub> /V <sub>2</sub> ) | Calculated  | Total   |
| mg/kg   | µg/kg   | µg/kg       | mg/kg  | µg/kg   | µg/kg       |         |
| 2hrs  | T = 3.68  | 22          | 28.38  | T = 21.1  | 116.19      | 126.32  |
|   | B = 1.03  | 6.38        |        | B = 1.84  | 10.13       |         |
|   | V <sub>1</sub> = 45855.04<br>V <sub>2</sub> = 45871.18                      | ΔV = 16.14  |        | V <sub>1</sub> = 13896.09<br>V <sub>2</sub> = 13914.25                      | ΔV = 18.16  |         |
| 5hrs  | T= 6.48   | 15.28       | 17.71  | T= 6.01   | 12.28       | 7.38    |
|   | B= 1.03   | 2.43        |        | B= 1.37   | 2.798       |         |
|   | V <sub>1</sub> = 45871.45<br>V <sub>2</sub> = 45913.86                      | ΔV = 42.41  |        | V <sub>1</sub> = 13914.46<br>V <sub>2</sub> = 13963.41                      | ΔV = 48.95  |         |
| 8hrs  | T= 4.94   | 7.23        | 8.94   | T= 7.41   | 8.40        | 10.06   |
|   | B= 1.17   | 1.71        |        | B= 1.46   | 1.66        |         |
|   | V <sub>1</sub> = 45913.80<br>V <sub>2</sub> = 45982.10                      | Δ V = 68.3  |        | V <sub>1</sub> = 13963.39<br>V <sub>2</sub> =14051.585                      | ΔV = 88.195 |         |
| 16hrs   | T= 16.1   | 8.95        | 10.17  | T= 1.17   | 0.569       | 1.119   |
|   | B= 2.2  | 1.22        |        | B= 1.4  | 0.55        |         |
|   | V <sub>1</sub> = 45982.83<br>V <sub>2</sub> = 46162.67                      | ΔV = 179.84 |        | V <sub>1</sub> = 14052.24<br>V <sub>2</sub> = 14257.77                      | ΔV = 205.53 |         |
| 24hrs   | T= 276.5  | 122.77      | 123.53 | T= 188.2  | 103.55      | 104.848 |
|   | B= 1.72   | 0.76        |        | B= 2.36   | 1.298       |         |
|   | V <sub>1</sub> = 46162.67<br>V <sub>2</sub> = 46387.89                      | ΔV = 225.22 |        | V <sub>1</sub> = 14257.77<br>V <sub>2</sub> = 14439.52                      | ΔV = 181.75 |         |
| 48 hrs, which was until 30% reactor power was reached | T= 37   | 11.21       | 11.58  | T= 20.25  | 16.89       | 88.64   |
|   | B = 1.23  | 0.37        |        | B = 86  | 71.75       |         |
|   | V <sub>1</sub> = 46387.89<br>V <sub>2</sub> = 46717.89                      | ΔV = 330    |        | V <sub>1</sub> = 14439.52<br>V <sub>2</sub> =14559.38                       | ΔV = 119.86 |         |

**T = Top filter B = Bottom filter**



## 5.2 Pictures of filter samples

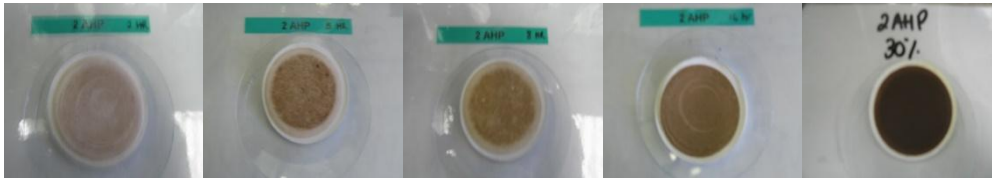


Figure 5.1: Pictures of filter AHP2 samples

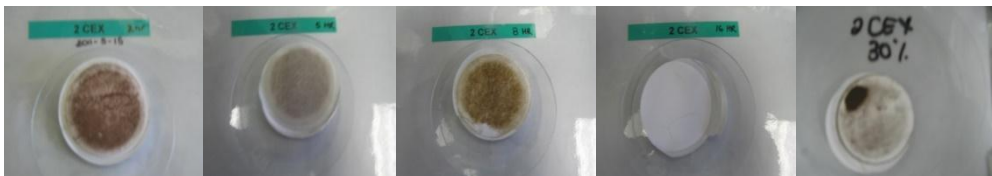


Figure 5.2: Pictures of 2CEX filter samples

Sample filters were photographed as they were being retrieved as per the standard operating procedure, however it was discovered that the picture for the 24 hrs sample filter was missing. It was either not photographed or the picture went missing because the analysts could not account for it, this is why it is not included in the sequences in Figure 5.1 and Figure 5.2, but its results are reflected in Table 5.1 and happens to be the peaks observed in both Figures 5.3 and Figure 5.4.

From the pictures in Figure 5.2 for the CEX system, the colour intensity drops from the 2 hrs sampling period to the 5 hrs sampling period, which correlates with the decrease observed in the data from  $116 \mu\text{g/kg}$  –  $12.28 \mu\text{g/kg}$  (particulate) and further to  $0.569 \mu\text{g/kg}$ . It is interesting to note that the soluble and particulate fraction amounts are almost the same,  $0.569 \mu\text{g/kg}$  compared with  $0.55 \mu\text{g/kg}$  at the 16 hrs point, and that there are no visible particulates on the filter.

It could be that the top filter was not placed correctly, possibly upside down because the volume indicates that there was sample flow through the filters. Also, there is a significant increase in the soluble iron amount at a 46 hrs point, with an accompanied drop in particulate amounts, this could indicate a chemistry effect of low pH in this low temperature region accompanied by oxidative conditions of dissolving particulate oxides into soluble ferrous ions, this is supported by visual indication on the filter paper whereby only a small particulate accumulation appears.

The intermediate colour of the filters for both systems at the beginning is light brownish and gets black at 30 % reactor power, this could be indication of the evolution of particulates from hematite ( $\text{Fe}_2\text{O}_3$ ) and/or oxyhydrate (particularly  $\gamma\text{-FeOOH}$ ) to magnetite ( $\text{Fe}_3\text{O}_4$ ) during a

transition from oxidative conditions due to low hydrazine concentration towards reducing conditions as hydrazine is increased with a related decrease in the dissolved oxygen. This observation is consistent with what is reported by Sawick, J.A et al. (2011:473) that high levels of  $\gamma$ -FeOOH were observed in one startup, suggesting that active corrosion is still occurring.

The calculated  $\mu\text{g/kg}$  results in Table 5.1 above are calculated according to the following calculation:

$$[\text{Fe}] (\mu\text{g/l}) = [\text{result (mg/kg)} / 10] / \text{Vol}] \times 1000$$

**Equation 5.1**

Where:

- Result is the concentration obtained from the A.A in mg/kg
- Vol. is the volume of sample passed through the corrosion product sampler as follows, [Volume (l) in 4.2.4.3 - Volume (l) in 4.2.3.10]

The total iron concentration is as per the following equation:

$$\text{Result (soluble)} + \text{Result (insoluble)} = \text{Total (Fe)}$$

**Equation 5.2**

**5.3 Graphical representation of data**

Below are graphical representations of iron results from Table 5.1 above.

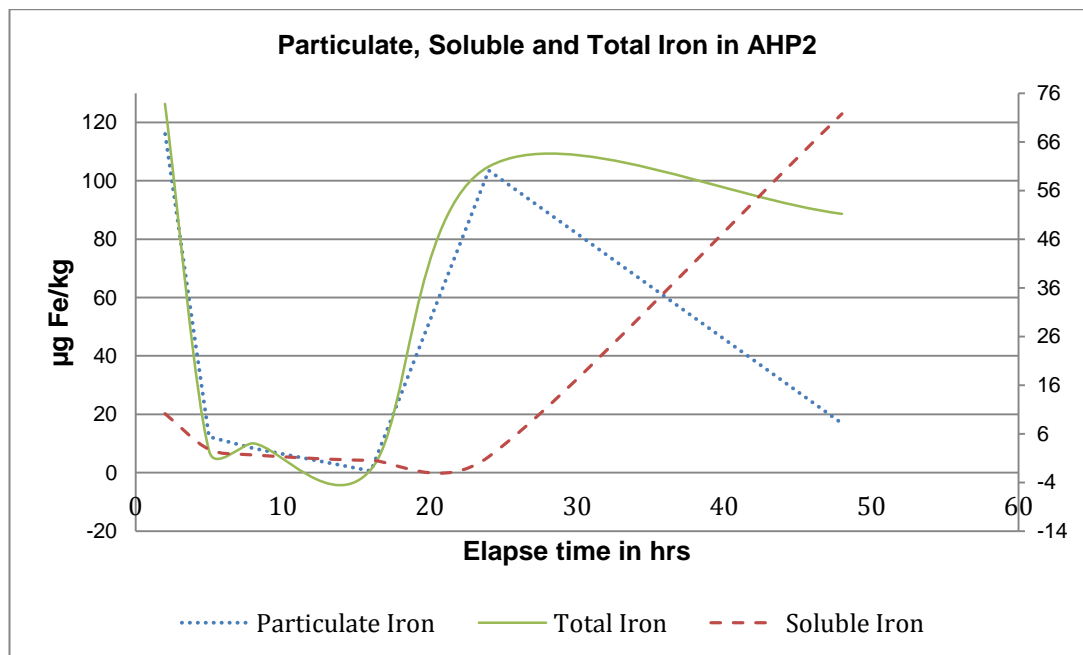


**Figure 5.3: Graphical representation of particulate vs. soluble iron concentrations for AHP2**

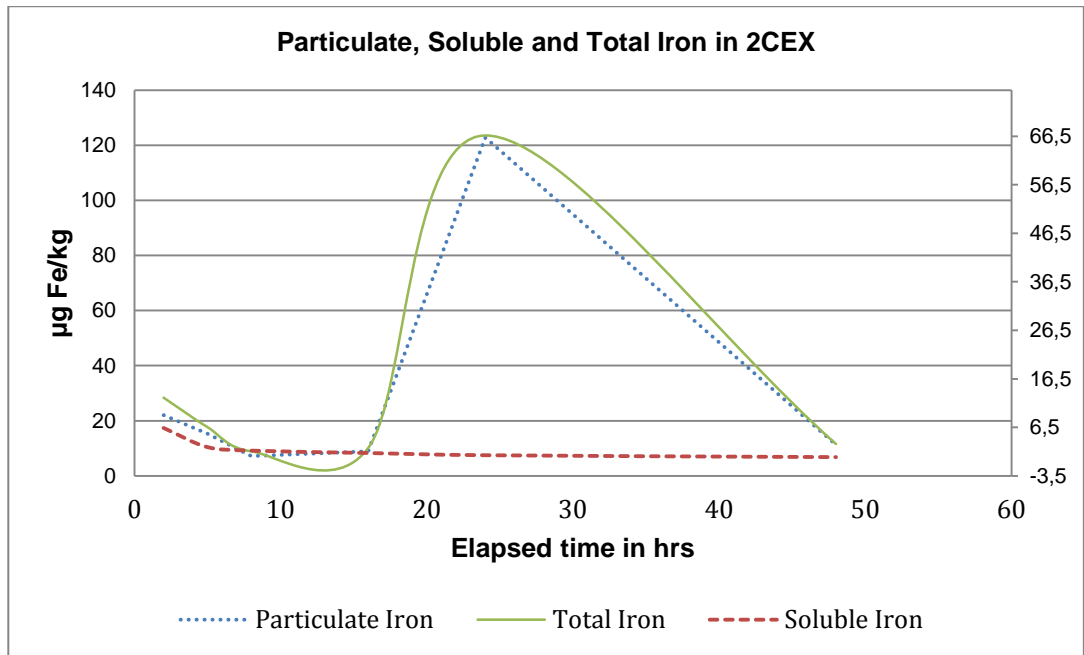


**Figure 5.4: Graphical representation of particulate vs. soluble iron concentrations for 2CEX**

A peak in iron at the 24 hrs point could be due to hydrodynamic effects caused by the starting of a condensate extraction pump. The fact that the peak is observed in both 2CEX and AHP2 systems supports the suggestion that this is not an out of trend data point given that both systems are in series with one another and occurred at the same time.

#### 5.4 Transport calculations

The following transport expression was used to perform transport calculations

$$T = 10^{-11} \times C \times W_{fw} \times \%P \times \Delta t.$$

##### Equation 5.3

- T is the quantity of iron transported by feedwater during sampling period, kg
- C is measured concentration, µg/kg
- $W_{fw}$  is feedwater flow rate at full power, kg/hour (5400 t/hr for AHP2 and 1800 t/hr for 2CEX)
- %P is percent power (average during sampling period)
- $\Delta t$  is sampling period, hours
- $10^{-11}$  is a unit's conversion factor

The calculated transport values are given in Table 5.2 with an example given below for AHP2 with the following conditions:

- C = 28.38 µg Fe/kg
- $W_{fw} = 5400$  t/hr
- %P = 12 %
- $\Delta t = 2$  hrs

$$T = 10^{-11} \times 28.38 \times 5400000 \times 12 \times 2 \text{ µg/kg.kg/hr.hr}$$

$$= 0.04 \text{ kg}$$

**Table 5.2: Transport amounts as calculated for less than 30 % reactor power and 11 days basis of up to 100 % reactor power**

| AHP2                     |                   |                                 | 2CEX  |   |                          |
|--------------------------|-------------------|---------------------------------|---|---|--------------------------|
| Sampling period, hrs     | [Fe] total, µg/kg | Calculated Transport amount, kg | [Fe] total, µg/kg                                     | Calculated Transport amount, kg           | Average Reactor power, % |
| 2                        | 28.38             | 0.04                            | 126.32  | 0.06                                      | 12                       |
| 5                        | 17.71             | 0.08                            | 7.38  | 0.01                                      | 16                       |
| 8                        | 8.94              | 0.08                            | 10.06   | 0.03                                      | 20                       |
| 16                       | 10.17             | 0.22                            | 1.119   | 0.01                                      | 25                       |
| 24                       | 123.53            | 4.48                            | 104.85  | 1.32                                      | 28                       |
| 46                       | 11.58             | 0.86                            | 88.64   | 2.30                                      | 30                       |
| Total                    |                   | 5.76                            |   | 3.73                                      |                          |
|                          |                   |                                 |   |   |                          |
| 4days                    | 5.4482            | 2.31                            |   |   | 47                       |
| 7days                    | 3.5538            | 1.77                            |   |   | 55                       |
|                          |                   |                                 | % of actual sludge amount of 38 kg for the fuel cycle | % of estimated fuel cycle amount of 72 kg |                          |
| Total (11 days)          |                   | 4.08                            | 11  | 6   |                          |
| Total (< 30 % + 11 days) |                   | 9.84                            | 26  | 14  |                          |

A difference of 2.03 kg is observed between AHP2 (5.76 kg) and CEX (3.73 kg) transport amounts, which could suggest that the 2.03 kg emanates from the intervening feedheaters and the related pipe work given that at this point of the startup, the forward drains pump was not yet started. However, if the 2.03 kg does not emanate from the intervening feed heaters and the related pipe work, this would imply that it comes directly from AHP feed heaters alone, or that both AHP together with the intervening feedheaters and pipe work contributed to that total amount of 2.03 kg.

This point cannot be verified as no sampling was done in between the two systems given that there are no sampling facilities and that identifying points of origin was not part of the study. It is worth noting that the 3.73 kg for CEX and 5.76 kg for AHP2 works out to 9.49 kg compared to the estimated total amount of 9.84 kg, which confirms that the CEX system also contributes to the transported total amount.

It should be noted that the total transport amount of 9.84 kg is for cycle number 18 in Figure 3.1, for which the retrieved total mass of sludge is 38 kg. Therefore, the startup amount of 9.84 Kg represents 26 % of the total mass of sludge for that fuel cycle.

Cycle data together with the calculated transport amounts following the startup for the entire fuel cycle is as per Table 6.3 below. In this case equation 5.3 becomes,

$$T = 10^{-9} \times C \times W_{fw} \times \Delta t \text{ because the average reactor power is 100 \% .}$$

#### Equation 5.4

**Table 5.3: AHP2 Iron data for 100 % reactor power and the whole fuel cycle**

| Date       | Fe(total)<br>µg/kg | Calculated<br>transport<br>amount, kg | Date       | Fe(total)<br>µg/kg | Calculated<br>Transport<br>amount, kg | Date       | Fe(total)<br>µg/kg | Calculated<br>transport<br>amount, kg |
|------------|--------------------|---------------------------------------|------------|--------------------|---------------------------------------|------------|--------------------|---------------------------------------|
| 2011/05/30 | 3,069              | 2.784                                 | 2012/01/30 | 0,873              | 0,792                                 | 2012/08/20 | 1,3956             | 1,266                                 |
| 2011/06/06 | 1,082              | 0.981                                 | 2012/02/06 | 1,635              | 1,484                                 | 2012/08/27 | 0,8028             | 0,728                                 |
| 2011/06/13 | 1,514              | 1.373                                 | 2012/02/13 | 0,889              | 0,806                                 | 2012/09/03 | 1,3274             | 1,204                                 |
| 2011/06/20 | 0,743              | 0,674                                 | 2012/02/20 | 0,954              | 0,866                                 |            |                    |                                       |
| 2011/06/27 | 1,022              | 0,927                                 | 2012/02/27 | 0,959              | 0,870                                 |            |                    |                                       |
| 2011/07/04 | 1,325              | 0,803                                 | 2012/03/05 | 1,067              | 0,968                                 |            |                    |                                       |
| 2011/07/11 | 0,886              | 0,986                                 | 2012/03/12 | 1,109              | 1,006                                 |            |                    |                                       |
| 2011/07/18 | 1,087              | 1,043                                 | 2012/03/19 | 1,324              | 1,201                                 |            |                    |                                       |
| 2011/07/25 | 1,149              | 1,328                                 | 2012/03/26 | 0,982              | 0,890                                 |            |                    |                                       |
| 2011/08/01 | 1,464              | 1,459                                 | 2012/04/02 | 1,056              | 0,958                                 |            |                    |                                       |
| 2011/08/08 | 1,608              | 1,079                                 | 2012/04/09 | 1,219              | 1,105                                 |            |                    |                                       |
| 2011/08/15 | 1,180              | 1,130                                 | 2012/04/16 | 0,887              | 0,805                                 |            |                    |                                       |
| 2011/08/22 | 1,246              | 0,872                                 | 2012/04/23 | 0,9672             | 0,877                                 |            |                    |                                       |
| 2011/08/29 | 0,962              | 1,751                                 | 2012/04/30 | 0,9524             | 0,864                                 |            |                    |                                       |
| 2011/09/12 | 1,920              | 1,962                                 | 2012/05/07 | 1,0297             | 0,934                                 |            |                    |                                       |
| 2011/09/19 | 2,162              | 1,659                                 | 2012/05/14 | 1,5026             | 1,363                                 |            |                    |                                       |
| 2011/09/26 | 1,829              | 1,673                                 | 2012/05/21 | 1,0808             | 0,981                                 |            |                    |                                       |
| 2011/10/03 | 1,844              | 0,967                                 | 2012/05/28 | 1,0382             | 0,942                                 |            |                    |                                       |
| 2011/10/10 | 1,066              | 1,507                                 | 2012/06/04 | 1,3182             | 1,196                                 |            |                    |                                       |
| 2011/10/17 | 1,661              | 1,571                                 | 2012/06/11 | 1,199              | 1,088                                 |            |                    |                                       |
| 2011/12/05 | 1,732              | 1,307                                 | 2012/06/18 | 1,0745             | 0,975                                 |            |                    |                                       |
| 2011/12/12 | 1,441              | 1,112                                 | 2012/06/25 | 1,0916             | 0,990                                 |            |                    |                                       |
| 2011/12/19 | 1,225              | 1,479                                 | 2012/07/02 | 1,076              | 0,976                                 |            |                    |                                       |
| 2011/12/26 | 1,63               | 1,347                                 | 2012/07/09 | 0,6928             | 0,629                                 |            |                    |                                       |
| 2012/01/03 | 1,485              | 1,456                                 | 2012/07/16 | 1,1498             | 1,043                                 |            |                    |                                       |
| 2012/01/09 | 1,605              | 1,456                                 | 2012/07/23 | 1,0656             | 0,967                                 |            |                    |                                       |
| 2012/01/16 | 1,476              | 1,339                                 | 2012/08/06 | 1,0096             | 0,916                                 |            |                    |                                       |
| 2012/01/23 | 1,608              | 1,459                                 | 2012/08/13 | 1,1468             | 1,040                                 |            |                    |                                       |

# CHAPTER 6

## DATA TREATMENT

### 6.1 Data treatment and statistics

**Table 6.1: Tabulation of cumulative amounts and inputs into the regression expression**

| y<br>CTA,<br>kg | x <sub>i</sub><br>time,<br>hrs | y <sub>i</sub><br>CA, kg | y<br>CTA,<br>kg | x <sub>i</sub><br>time,<br>hrs | y <sub>i</sub><br>CA, kg | x <sub>i</sub> y <sub>i</sub><br>hrs * kg | x <sub>i</sub> <sup>2</sup><br>time, hrs | y <sup>2</sup><br>CA, kg | x <sub>i</sub> y <sub>i</sub><br>hrs * kg | x <sub>i</sub> <sup>2</sup><br>time, hrs | y <sup>2</sup><br>CA, kg |
|-----------------|--------------------------------|--------------------------|-----------------|--------------------------------|--------------------------|---|--|--------------------------|---|--|--------------------------|
| 2.310           | 96                             | 2.310                    | 1.006           | 6144                           | 48.356                   | 222                                       | 9216                                     | 5.3351                   | 297099                                    | 37748736                                 | 2338.303                 |
| 1.770           | 264                            | 4.080                    | 1.201           | 6312                           | 49.557                   | 1077                                      | 69696                                    | 16.6464                  | 312804                                    | 39841344                                 | 2455.896                 |
| 2.784           | 432                            | 6.864                    | 0.890           | 6480                           | 50.447                   | 2965                                      | 186624                                   | 47.1145                  | 326897                                    | 41990400                                 | 2544.899                 |
| 0.981           | 600                            | 7.845                    | 0.958           | 6648                           | 51.405                   | 4707                                      | 360000                                   | 61.544                   | 341740                                    | 44195904                                 | 2642.474                 |
| 1.373           | 768                            | 9.218                    | 1.105           | 6816                           | 52.51                    | 7079                                      | 589824                                   | 84.972                   | 357908                                    | 46457856                                 | 2757.300                 |
| 0.674           | 936                            | 9.892                    | 0.805           | 6984                           | 53.315                   | 9259                                      | 876096                                   | 97.852                   | 372352                                    | 48776256                                 | 2842.489                 |
| 0.927           | 1104                           | 10.819                   | 0.877           | 7152                           | 54.192                   | 11944                                     | 1218816                                  | 117.051                  | 387581                                    | 51151104                                 | 2936.773                 |
| 0.803           | 1272                           | 11.622                   | 0.864           | 7320                           | 55.056                   | 14783                                     | 1617984                                  | 135.071                  | 403010                                    | 53582400                                 | 3031.163                 |
| 0.986           | 1440                           | 12.608                   | 0.934           | 7488                           | 55.99                    | 18156                                     | 2073600                                  | 158.962                  | 419253                                    | 56070144                                 | 3134.880                 |
| 1.043           | 1608                           | 13.651                   | 1.363           | 7656                           | 57.353                   | 21951                                     | 2585664                                  | 186.3498                 | 439095                                    | 58614336                                 | 3289.367                 |
| 1.328           | 1776                           | 14.979                   | 0.981           | 7824                           | 58.334                   | 26603                                     | 3154176                                  | 224.370                  | 456405                                    | 61214976                                 | 3402.856                 |
| 1.459           | 1944                           | 16.438                   | 0.942           | 7992                           | 59.276                   | 31955                                     | 3779136                                  | 270.2078                 | 473734                                    | 63872064                                 | 3513.644                 |
| 1.079           | 2112                           | 17.517                   | 1.196           | 8160                           | 60.472                   | 36996                                     | 4460544                                  | 306.845                  | 493452                                    | 66585600                                 | 3656.863                 |
| 1.130           | 2280                           | 18.647                   | 1.088           | 8328                           | 61.56                    | 42515                                     | 5198400                                  | 347.711                  | 512672                                    | 69355584                                 | 3789.634                 |
| 0.872           | 2448                           | 19.519                   | 0.975           | 8496                           | 62.535                   | 47783                                     | 5992704                                  | 380.991                  | 531297                                    | 72182016                                 | 3910.626                 |
| 1.751           | 2616                           | 21.270                   | 0.990           | 8664                           | 63.525                   | 55642                                     | 6843456                                  | 452.413                  | 550381                                    | 75064896                                 | 4035.425                 |
| 1.962           | 2784                           | 23.232                   | 0.976           | 8832                           | 64.501                   | 64678                                     | 7750656                                  | 539.725                  | 569673                                    | 78004224                                 | 4160.379                 |
| 1.659           | 2952                           | 24.891                   | 0.629           | 9000                           | 65.13                    | 73478                                     | 8714304                                  | 619.562                  | 586170                                    | 81000000                                 | 4241.917                 |
| 1.673           | 3120                           | 26.564                   | 1.043           | 9168                           | 66.173                   | 82880                                     | 9734400                                  | 705.646                  | 606674                                    | 84052224                                 | 4378.865                 |
| 0.967           | 3288                           | 27.531                   | 0.967           | 9336                           | 67.14                    | 90522                                     | 10810944                                 | 757.956                  | 626819                                    | 87160896                                 | 4507.780                 |
| 1.507           | 3456                           | 29.038                   | 0.916           | 9504                           | 68.056                   | 100355                                    | 11943936                                 | 843.205                  | 646804                                    | 90326016                                 | 4631.619                 |
| 1.571           | 3624                           | 30.609                   | 1.040           | 9672                           | 69.096                   | 110927                                    | 13133376                                 | 936.911                  | 668297                                    | 93547584                                 | 4774.257                 |
| 1.307           | 3792                           | 31.916                   | 1.266           | 9840                           | 70.362                   | 121025                                    | 14379264                                 | 1018.631                 | 692362                                    | 96825600                                 | 4950.811                 |
| 1.112           | 3960                           | 33.028                   | 0.728           | 10008                          | 71.09                    | 130790                                    | 15681600                                 | 1090.849                 | 711469                                    | 100160064                                | 5053.788                 |
| 1.479           | 4120                           | 34.507                   | 1.204           | 10176                          | 72.294                   | 142168                                    | 16974400                                 | 1190.733                 | 735664                                    | 103550976                                | 5226.422                 |
| 1.347           | 4296                           | 35.854                   |                 |                                |                          | 154028                                    | 18455616                                 | 1285.509                 |   |  |                          |
| 1.456           | 4464                           | 37.310                   |                 | $\Sigma x_i$                   | $\Sigma y_i$             | 166551                                    | 19927296                                 | 1392.0361                | $\Sigma x_i y_i$                          | $\Sigma x_i^2$                           | $\Sigma y_i^2$           |
| 1.456           | 4632                           | 38.766                   |                 | <b>313288</b>                  | <b>2430.010</b>          | 179564                                    | 21455424                                 | 1502.803                 | <b>16054902</b>                           | <b>2142818112</b>                        | <b>122495.310</b>        |
| 1.339           | 4800                           | 40.105                   |                 |                                |                          | 192504                                    | 23040000                                 | 1608.411                 |   |  |                          |
| 1.459           | 4968                           | 41.564                   |                 |                                |                          | 206489                                    | 24681024                                 | 1727.566                 |   |  |                          |
| 0.792           | 5136                           | 42.356                   |                 |                                |                          | 217540                                    | 26378496                                 | 1794.031                 |   |  |                          |
| 1.484           | 5304                           | 43.84                    |                 |                                |                          | 232527                                    | 28132416                                 | 1921.9456                |   |  |                          |
| 0.806           | 5472                           | 44.646                   |                 |                                |                          | 244302                                    | 29942784                                 | 1993.265                 |   |  |                          |
| 0.866           | 5640                           | 45.512                   |                 |                                |                          | 256687                                    | 31809600                                 | 2071.342                 |   |  |                          |
| 0.870           | 5808                           | 46.382                   |                 |                                |                          | 269386                                    | 33732864                                 | 2151.2899                |   |  |                          |
| 0.968           | 5976                           | 47.350                   |                 |                                |                          | 282964                                    | 35712576                                 | 2242.0225                |   |  |                          |

The next step was to plot a curve of cumulative amounts of iron as a function of time for the entire fuel cycle; the cumulative amounts were worked out from the calculated transport amounts. From the plotted curve, a method of least squares was then used to find the best fit line or regression line through the data from which the amount (kg) at time zero ( $x_i = 0$ ) was estimated.

From Table 6.1, data for  $x_i$  and  $y_i$  is used to plot the flowing cumulative curve in which the best fit or regression line is drawn as indicated in the curve.

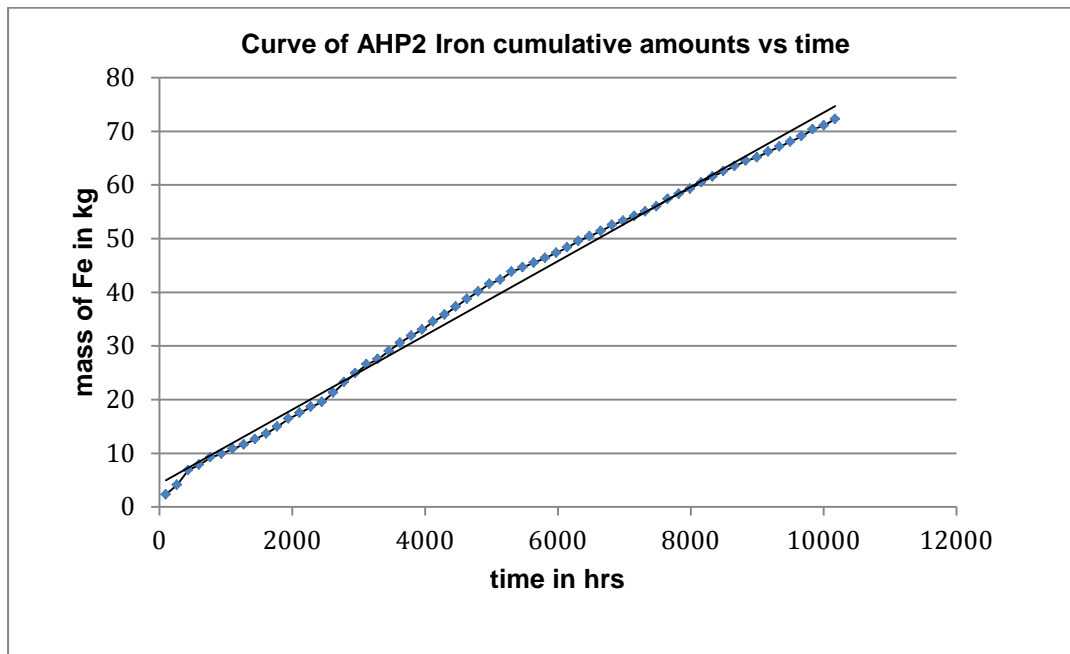


Figure 6.1: Curve of cumulative iron amounts

The best fit line through the data follows the following equation:

$$y = a + bx$$

**Equation 6.1**

Where,

$$a = \frac{(\sum y_i)(\sum x_i^2) - (\sum x_i)(\sum x_i y_i)}{n(\sum x_i^2) - (\sum x_i)^2}$$

**Equation 6.2**

$$b = \frac{n(\sum x_i y_i) - (\sum x_i)(\sum y_i)}{n(\sum x_i^2) - (\sum x_i)^2}$$

**Equation 6.3**



Both a and b are calculated as follows from the data in Table 6.1,

$$a = \frac{(2430.010)(2142818112) - (313288)(16054902)}{61(2142818112) - (313288)^2}$$

$$= 5.443$$

$$b = \frac{61(16054902) - (313288)(2430.010)}{61(2142818112) - (313288)^2}$$

$$= 0.0067$$

Therefore, the regression equation for the best fit line through the data is,

$$y = 5.443 + 0.00669x$$

#### Equation 6.4

The predicted intercept (y, kg) at  $x_i (t_0) = 0$  is 5.443 kg

The amount based on collected samples < 30 % reactor power being time zero as defined is 5.76 kg, see Table 5.2.

Given the dynamic nature of the start-up, it is difficult to replicate the samples below 30 % reactor power, therefore it is not possible to do a statistical comparison of the two values due to this limitation.

We then work out the regression coefficient to test whether the regression model fits the data

$$r = \frac{n(\sum xy) - (\sum x)(\sum y)}{\sqrt{[n\sum x^2 - (\sum x)^2][n\sum y^2 - (\sum y)^2]}}$$

$$r = \frac{61(16054901.88) - (313288)(2430.01)}{\sqrt{[61 \cdot 2142818112 - (313288)^2][61 \cdot 122495.31 - (2430.01)^2]}}$$

$$= 0.9653$$

$$r^2 = 0.932$$

This  $r^2$  value means that about 93 % of the data points lie on the regression line, which indicates that the regression model fits the data. This can be attributed to the large amount of data collected for the purpose of constructing a cumulative curve, indicating that the errors are reduced with an increase in data points.

The final step is to express the standard error of the estimate as follows,

$$s = \sqrt{\frac{\sum(y_i - y_p)^2}{N}}$$

**Equation 6.5**

Where,

- $y_i$  is the observed value
- $y_p$  is the predicted value according to the regression equation
- N is the number of paired observations

**Table 6.2: Tabulation of inputs into the standard error expression**

| $y_i$<br>Cumulative<br>amount,<br>kg | $y_p$<br>Predicted<br>amount,<br>kg | $y_i - y_p$ | $(y_i - y_p)^2$ | $y_i$  | $y_p$  | $y_i - y_p$ | $(y_i - y_p)^2$       |
|--------------------------------------|-------------------------------------|-------------|-----------------|--------|--------|-------------|-----------------------|
| 2.310                                | 6.085                               | -3.775      | 14.252          | 48.356 | 46.546 | 1.810       | 3.275                 |
| 4.080                                | 7.209                               | -3.129      | 9.792           | 49.557 | 47.670 | 1.887       | 3.561                 |
| 6.864                                | 8.423                               | -1.560      | 2.433           | 50.447 | 48.794 | 1.653       | 2.732                 |
| 7.845                                | 9.583                               | -1.738      | 3.021           | 51.405 | 49.918 | 1.487       | 2.211                 |
| 9.218                                | 10.742                              | -1.524      | 2.322           | 52.510 | 52.473 | 0.0366      | 0.001                 |
| 9.892                                | 11.901                              | -2.009      | 4.036           | 53.315 | 53.633 | -0.318      | 0.101                 |
| 10.819                               | 13.061                              | -2.242      | 5.025           | 54.192 | 53.290 | 0.902       | 0.814                 |
| 11.622                               | 13.584                              | -1.962      | 3.848           | 55.056 | 54.414 | 0.642       | 0.412                 |
| 12.608                               | 15.379                              | -2.771      | 7.678           | 55.990 | 57.110 | -1.120      | 1.255                 |
| 13.651                               | 16.538                              | -2.887      | 8.336           | 57.353 | 58.269 | -0.916      | 0.839                 |
| 14.979                               | 17.697                              | -2.718      | 7.390           | 58.334 | 57.786 | 0.548       | 0.300                 |
| 16.438                               | 18.857                              | -2.419      | 5.850           | 59.276 | 58.909 | 0.367       | 0.135                 |
| 17.517                               | 20.016                              | -2.499      | 6.244           | 60.472 | 61.747 | -1.275      | 1.626                 |
| 18.647                               | 21.175                              | -2.528      | 6.391           | 61.560 | 62.906 | -1.346      | 1.812                 |
| 19.519                               | 22.334                              | -2.815      | 7.925           | 62.535 | 62.281 | 0.254       | 0.065                 |
| 21,270                               | 23.493                              | -2.224      | 4.945           | 63.525 | 63.405 | 0.120       | 0.014                 |
| 23.232                               | 24.653                              | -1.421      | 2.018           | 64.501 | 64.529 | -0.028      | 0.001                 |
| 24.891                               | 25.812                              | -0.921      | 0.848           | 65.130 | 65.653 | -0.523      | 0.274                 |
| 26.564                               | 26.971                              | -0.407      | 0.166           | 66.173 | 66.777 | -0.604      | 0.365                 |
| 27.531                               | 28.130                              | -0.599      | 0.359           | 67.140 | 67.900 | -0.761      | 0.579                 |
| 29.038                               | 29.289                              | -0.251      | 0.063           | 68.056 | 69.025 | -0.969      | 0.939                 |
| 30.609                               | 30.449                              | 0.160       | 0.026           | 69.096 | 70.149 | -1.053      | 1.109                 |
| 31.916                               | 31.608                              | 0.308       | 0.095           | 70.362 | 71.273 | -0.911      | 0.829                 |
| 33.028                               | 32.767                              | 0.261       | 0.068           | 71.090 | 72.397 | -1.307      | 1.708                 |
| 34.507                               | 33.871                              | 0.636       | 0.404           | 72.294 | 75.657 | -3.363      | 11.310                |
| 35.854                               | 35.085                              | 0.769       | 0.591           |        |        |             |                       |
| 37.310                               | 36.245                              | 1.065       | 1.135           |        |        |             | $\Sigma(y_i - y_p)^2$ |
| 38.766                               | 37.404                              | 1.362       | 1.856           |        |        |             | <b>178.171</b>        |
| 40.105                               | 38.563                              | 1.542       | 2.378           |        |        |             |                       |
| 41.564                               | 38.679                              | 2.885       | 8.885           |        |        |             |                       |
| 42.356                               | 40.881                              | 1.475       | 2.174           |        |        |             |                       |
| 43.840                               | 40.927                              | 2.913       | 8.486           |        |        |             |                       |
| 44.646                               | 42.051                              | 2.595       | 6.736           |        |        |             |                       |
| 45.512                               | 44.359                              | 1.153       | 1.329           |        |        |             |                       |
| 46.382                               | 44.299                              | 2.084       | 4.341           |        |        |             |                       |
| 47.350                               | 46.677                              | 0.673       | 0.452           |        |        |             |                       |

Therefore, from the data in Table 6.2, the standard error works out as follows:

$$s = \sqrt{\frac{178.171}{61}}$$

= 1.709, which indicates the precision of the prediction.

Therefore, this value tells us that the predicted values from the regression line will fall within +/- 1.709 response units. So, the 5.443 kg predicted value at time zero ( $x_i$ ) will be precise within the 3.734 – 7.152 range. This represents 31 % standard error of the estimate.

## CHAPTER 7

### CONCLUSIONS

#### 7.1 Conclusions

The iron concentration values during the startup phase were found to range from 8.94 µg/kg to 17.71 µg/kg with an average of 16.58 µg/kg. The expected value as hypothesised was about 10 µg/kg, which is in line with the obtained values.

In terms of how the startup concentration values below 30 % reactor power compares with those above 30 % until 100 % reactor power, it was found that the concentrations decreases as the reactor power exceeds 30 % and remains relatively stable as the unit reaches steady state conditions once 100 % is reached. Even though the measured concentration values are high below 30 % reactor power, the actual transport amount values are lower compared to those at higher reactor power with lower concentration values. This due to the difference in flow rates, which supports the fact that most of the iron is transported at higher reactor power levels during steady state operation.

Based on the concentration values obtained during the study for the entire fuel cycle, transport amounts were calculated to enable the construction of a cumulative curve from which the startup transport amount for reactor less than 30 % was estimated based on the regression model and found to be 5.443 kg. The transport amount based on the actual samples for the same window was found to be 5.76 kg. However, the total amount of transported corrosion products for startup including the 11 days startup basis is 9.84 kg, which represents 26 % of the total cycle mass retrieved from the steam generators following the fuel cycle after this study.

Although it is difficult to pinpoint the exact effectiveness of the chemistry, the indication from literature is that increased transport amounts during startup can be attributed to chemistry parameters such as oxygen, pH and hydrazine. It can therefore be said that it is important to establish both reducing and elevated pH conditions in the feedwater as early as practicably possible during plant startup, this is to minimize dissolution of particulate iron oxide and also to promote magnetite ( $\text{Fe}_3\text{O}_4$ ) formation. This is important because it is estimated that the kinetics of iron oxide reduction by hydrazine ( $\text{N}_2\text{H}_4$ ) takes about 4 hrs to convert lepidocrocite of various morphologies to 100 % magnetite at 150 °C [33], lepidocrocite is reportedly the dominant oxyhydroxide existing at startup.

From literature review, the reported amounts of transported corrosion products are in the range of 1.816 kg to 36.32 kg with a median value of about 6.81 kg. These ranges and the median compares well with the 9.84 kg amount found for Koeberg's cycle 18 on unit 2. This amount is deemed to be within industry norms across the nuclear industry. Therefore, in light of this and considering that the slope of the cumulative curve or the transport rate is 0.007 kg/hr, compared to the one case of 0.19 kg/hr as reported in the literature, it would seem that the current practices with respect to their effect on corrosion product transport are of no concern. Having said this however, it is still very difficult to make a conclusive statement given that the condenser water is cleaned prior to using the water to the steam generators to reduce turbidity, which is a measure of the solid in the water. So, most of the solids are removed and therefore not reflected in the results.

The estimated transport amount for the fuel cycle is 72 kg compared to the actual of 38 kg of sludge amount retrieved from the outage through sludge lancing. The difference is possibly due to the fact that the only sludge removed is that on the tube sheet given the square-pitch design of the tube bundles, and the inaccessible shadow areas behind the tubes where certain amount of sludge deposit remains and cannot be retrieved. The other mass would be accounted for by removal through the steam generator blowdown system whose flow rate is 45 t/hr for the entire fuel cycle, this amounts to an estimated average of about 1.3 kg of mass removal for the entire cycle.

If the sludge in the steam generators is not removed, it will continue to grow from one cycle to the next and will exacerbate tube fouling. Although sludge lancing is performed, the only sludge removed is that on the tube sheet given the square-pitch design of Koeberg's tube bundles. There are also inaccessible shadow areas behind the tubes where certain amount of sludge deposit remains [10]. Therefore, the sludge mass values depicted gives only estimates of the sludge deposited in the steam generators throughout a fuel cycle. Even with that, the information is still valuable in that it gives an indication of sludge accumulation from cycle to cycle.

## 7.2 Future work

This study conducted a once off evaluation of the transported amounts of corrosion products during a startup phase for a specific unit and fuel cycle, this means that the results and conclusions made are only limited to this unit and the fuel cycle in question. Therefore there is room to conduct more studies on a different unit and for different fuel cycles to gain further insight into the behaviour of corrosion products, which could assist in knowing whether the transport amounts are increasing, decreasing or staying the same from cycle to cycle and to try and understand the reasons.

Also, there is room for further work to be done in identifying the sources of corrosion products during plant startup. This could give insights into the status of material conditions in the different parts of the feedwater circuit. In addition to this, a mass balance could also be beneficial as a practice to monitor any system imbalances during startup, especially when the reactor power reaches 50 % and up to 100 %.

Furthermore, sampling condenser water (2CEX) before the water is cleaned through filtration and after could provide some information regarding the amounts that are distributed across the feedtrain when the water is on re-circulation prior to changing over to feeding the water directly to the steam generators and the effectiveness of clean-up by filtration. The normal practice is to determine the water turbidity after a period of cleaning up to check the water clarity before usage, the actual determination of iron could give better insight into iron behaviour.

## REFERENCES

1. Adenhorff, M.W. 1995. The use of ethanolamine at Koeberg. Eskom Internal Report.
2. Allie, M.N. 2011. Assessment Investigation Report, PR # 62067.
3. Anon. n.d. Feed train layout detail. Koeberg Training Presentation.
4. Anon. 1993. PWR Generic Fundamentals: Reactor Theory. Rev 1.
5. Anon. n.d. Secondary Chemistry Data Interpretation: Chemistry Training Course (KTC-CP-038).
6. Bonavigo, L. & De Salve, M. 2011. *Issues for Nuclear Power Plants Steam Generators*.
7. Comper, J.D. 2003. Conventional Island Chemical Sampling System: Koeberg Nuclear Power Station. NPO 1/2Module.
8. *Corrosion Product Transport during Boiling Water Reactor and Pressurized Water Reactor Startups*. EPRI, Palo Alto, CA: 2010. 1021112.
9. Douglas, D.L. 2007. *Corrosion and Wear Handbook for Water Cooled Reactors*. 6<sup>th</sup> ed. In Depaul, D.J. (ed). Fundamental Aspects of Iron Corrosion. USA: United States Atomic Energy Commission.
10. Eeden, N, & Galt, K.J. (2006). *Corrosion Product Sampling at Koeberg Nuclear Power Station*. Power Plant Chemistry, 8(3), 159-168.
11. *Effect of Oxygen Concentration on Corrosion Product Transport at South Texas Project Unit 1*, EPRI, Palo Alto, CA, and Houston Lighting and Power, Wadsworth, Texas: 2000. 1000742.
12. *Effect of Redox Conditions on Flow Accelerated Corrosion: Influence of Hydrazine and Oxygen*. EPRI, Palo Alto, CA, and Electricite de France, Moret Sur Loing, France: 2002. 1002768.
13. Fourie, S.P. 2008. Koeberg Chemistry: Primary and Secondary Plant Chemistry. Classroom Handout.
14. *Guidelines for Controlling Flow-accelerated Corrosion in Fossil and Combined Cycle Plants*. EPRI. Palo Alto. CA: 2005. 1008082.
15. *Guidelines for Controlling Flow-Accelerated Corrosion in Fossil and Combined Cycle Plants*, EPRI, Palo Alto, CA: 2005. 1008082.
16. Hammond, N. Cooling Water Chemistry. Corrosion Products and Their Effect on Accelerator Operation at the Diamond Light Source. Diamond Light Source Ltd.
17. Hearne, G.R. 2011. <sup>57</sup>Fe Mossbauer Analysis of Steam Generator Sludge: Outage 218. Mossbauer Laboratory C1-Lab144, Department of Physics University of Johannesburg.
18. Hook, T.A., Pearl, W.L. & Sawochka, S.G. 1987. *Corrosion-Product Transport in a Cycling Fossil Plant*. San Jose. EPRI.



19. Hudson-Lamb, D.C & Van Niekerk W.G. 2011. Test Report: Pelindaba Analytical Labs (Necsa). Pelindaba. Laboratory reference number: PS2011-1065/1. 08 June.
20. <https://www.chemguide.co.uk/inorganic/extraction/iron.html> [2017-12-17]
21. Makapela, G.A. 2012. Koeberg Chemistry. Chemistry Training Programs: Analytical Chemistry. Rev 3.
22. Martina, I., Wiesinger, R., Jembrih-Simburger, D. & Schreiner, M. 2012. *Micro-Raman Characterisation of Silver Corrosion Products: Instrument Set-up and Reference Database*. Scientific Research for the Preservation of Cultural Heritage.
23. Namduri, H. 2007. Formation and Quantification of Corrosion Deposits in the Power Industry. Unpublished Dissertation Prepared for the Degree of Doctor of Philosophy, University of Texas.
24. Odar, S & Nordmann, F. France. 2010. *PWR and VVER Secondary System Water Chemistry*. Stand Alone Report, Sweden, January 2010. Advanced Nuclear Technology International.
25. Pease, B.I., Michel, A., Stang, H. *Quantifying Movements of Corrosion Products in Reinforced Concrete using X-ray Attenuation Measurements*. 2<sup>nd</sup> International Conference on Microstructure Related Durability of Cementitious Composites (MicroDurability), Amsterdam, the Netherlands, 11-13 April, 2012.
26. Peters, N.J., Davidson, C.M., Britton, A. & Robertson, S.J. 1999. *The Nature of Corrosion Products in Lead Pipes Used to Supply Drinking Water to the City of Glasgow, Scotland, UK*. Fresenius' Journal of Analytical Chemistry, 363(5-6): 562-565. March.
27. *Pressurized Water Reactor Hideout Return Sourcebook: Prediction of Crevice Solution Chemistry in PWR Steam Generators*. EPRI, Palo Alto, CA: 2007. 1014985.
28. *Pressurized Water Reactor Primary Zinc Application Guidelines*. EPRI, Palo Alto, CA: 2006. 1013420.
29. *Pressurized Water Reactor Secondary Water Chemistry, Guidelines-Revision 7*. EPRI, Palo Alto, CA: 2009. 1016555.
30. Rhee, H., Jung, H. & Cho, D. 2014. *Evaluation of pH Control Agents Influencing on Corrosion of Carbon Steel in Secondary Water Chemistry Condition of Pressurized Water Reactor*. Nuclear Engineering and Technology.46(3):431-438. June.
31. Roonasi, P & Holmgren, A. A. 2009. *Study on the Mechanism of Magnetite Formation Based on Iron Isotope Fractionation*.
32. Sarin, P., Snoeyink, V.L., Lytle, D.A. & Kriven, W.M. 2004. *Iron Corrosion Scales: Model for Scale Growth, Iron Release, and Colored Water Formation*. Proceedings of the Environmental Engineering Conference, Niagara Falls, 22 July 2002. Journal of Environmental Engineering.
33. Sawick, J.A., Brett, M.E. & Tapping, R.L. *Corrosion-Product Transport, Oxidation State and Remedial Measures*. CA0000226. Third International Steam Generator and Heat Exchanger Conference, Toronto, June 1998. Canadian Nuclear Society.

34. Taylor, R.M. 1984. *Influence of Chloride on the Formation of Iron Oxides from Fe (II) Chloride. II. Effect of [Cl] on the Formation of Lepidocrocite and its Crystallinity*. Clays & Clay Minerals 32 (in press).
35. Van Eeden, N., Matthee, F.W. & Montshiwagae, M.M. 2012. *Experience and Optimization of Ethanolamine Treatment for a PWR Secondary System*. Proceedings of the 2012 International Nuclear Plant Chemistry Conference, Paris, 23-27 September 2012. French Nuclear Institute.
36. [www.eskom.co.za/aboutelectrocity/visitorcenters/pages/koeberg\\_power\\_station.aspx](http://www.eskom.co.za/aboutelectrocity/visitorcenters/pages/koeberg_power_station.aspx) [2017-12-17]
37. [www.sciencedirect.com/science/article/pii/S002954931300280X](http://www.sciencedirect.com/science/article/pii/S002954931300280X) [2017-12-17]
38. [www.wano.info/en-gb/aboutus/wanohistory](http://www.wano.info/en-gb/aboutus/wanohistory) [2017-12-17]
39. [www.world-nuclear.org/information-library/country-profiles/countries-o-s/south-africa.aspx](http://www.world-nuclear.org/information-library/country-profiles/countries-o-s/south-africa.aspx) [2017-12-17]

# APPENDIX A: RECOMMENDED CONDITIONS FOR FLAME ANALYSIS

## RECOMMENDED CONDITIONS – FLAME

Recommended Conditions

2011/09/06 02:36:55 PM Page 1

Element: Fe (Iron)

### Atomic Absorption

| Wavelength<br>(nm) | Slit Width<br>(nm) | Relative<br>Noise | Char. Conc<br>(mg/L) | Sensitivity<br>Check (mg/L) | Linear to<br>(mg/L) |
|--------------------|--------------------|-------------------|----------------------|-----------------------------|---------------------|
| 248.3              | 0.2                | 1                 | 0.1                  | 5                           | 5                   |
| 302.1              | 0.2                | 0.46              | 0.4                  | 20                          | 10                  |
| 305.9              | 0.2                | 0.4               | 2.4                  | 100                         |                     |
| 346.6              | 0.2                | 0.52              | 10                   | 500                         |                     |

Oxidant ..... 0.0  
Oxidant Flow (L/min) ..... 17.0  
Acetylene Flow (L/min) ..... 2.0

### Flame Emission

Wavelength (nm) ..... 372.0  
Slit (nm) ..... 0.2  
Oxidant ..... 0.0  
Oxidant Flow (L/min) ..... 16.0  
Acetylene Flow (L/min) ..... 7.8

### Remarks:

1. Data obtained with a standard nebulizer and flow spoiler.  
Operation with a high sensitivity nebulizer or one with an impact bead will typically provide a 2-3 X sensitivity improvement.
2. Check cookbook for possible interferences with multi-element lamps.
3. The signal is depressed slightly by Ni, Co, Cu & mineral acids.
4. Organic acids may reduce the signal.
5. Add 0.2% CaCl<sub>2</sub> to all solutions to overcome depression due to Si.

